MICROCOPY RESOLUTION TEST CHART
NATIONAL BUREAU OF STANDARDS 1963 A

AFOSR-TR- 79-0951

(III)

July 27, 1979

LEVEL II

Final Report

LASER FLUORESCENCE STUDIES OF
CHEMILUMINESCENT CHEMICAL REACTIONS

By: Graham Black

DDC
SEP 17 1979
RECEIVED
C

SRI International Project No. PYU-4273
Contract No. F44620-75-C-0083
Report MP 79-54

Prepared for:

AIR FORCE OFFICE OF SCIENTIFIC RESEARCH
Bolling Air Force Base, Building 410
Washington, D. C.   20332

Attention: Dr. Ralph Kelley

SRI International

AD A073829

DDC FILE COPY

SRI
International

333 Ravenswood Ave. • Menlo Park, California 94025
(415) 326-6200 • Cable: SRI INTL MPK • TWX: 910-373-1246

REPORT DOCUMENTATION PAGE		READ INSTRUCTIONS BEFORE COMPLETING FORM
1. REPORT NUMBER MP 79-54 AFOSR TR-79-0951	2. GOVT ACCESSION NO.	3. RECIPIENT'S CATALOG NUMBER
4. TITLE (and Subtitle) Laser Fluorescence Studies of Chemiluminescent Chemical Reactions		5. TYPE OF REPORT & PERIOD COVERED Final Report. June 1975 — July 1979
		6. PERFORMING ORG. REPORT NUMBER SRI-MP 79-54 SRI Proj. 4273
7. AUTHOR(s) Graham/Black		8. CONTRACT OR GRANT NUMBER(s) F44620-75-C-0083
9. PERFORMING ORGANIZATION NAME AND ADDRESS SRI International 333 Ravenswood Avenue Menlo Park, CA 94025		10. PROGRAM ELEMENT, PROJECT, TASK AREA & WORK UNIT NUMBERS 61102F 2301/A4
11. CONTROLLING OFFICE NAME AND ADDRESS Air Force Office of Scientific Research /NP Bolling Air Force Base, Building 410 Washington, D. C. 20332		12. REPORT DATE July 27, 1979 13. NUMBER OF PAGES 69
14. MONITORING AGENCY NAME & ADDRESS(if different from Controlling Office) F44620-75-C-0083		15. SECURITY CLASS. (of this report) Unclassified 15a. DECLASSIFICATION/DOWNGRADING SCHEDULE

16. DISTRIBUTION STATEMENT (of this Report)

Approved for public release; distribution unlimited.

27 Jul 79

17. DISTRIBUTION STATEMENT (of the abstract entered in Block 20, if different from Report)

70 p.

18. SUPPLEMENTARY NOTES

19. KEY WORDS (Continue on reverse side if necessary and identify by block number)

Vacuum ultraviolet photodissociation, $O(^1S)$ from N_2O, $S(^1S)$ from OCS, liquid argon and nitrogen, electronically excited XeF from XeF_2, radiative lifetimes, collisional rate coefficients.

20. ABSTRACT (Continue on reverse side if necessary and identify by block number)

Photodissociation of N_2O (to produce $O(^1S)$) and OCS (to produce $S(^1S)$) has been studied in liquid argon and nitrogen. Emission spectra and lifetime information have been obtained. Synchrotron radiation has been used to produce XeF (B, C, and D) states from XeF_2. Quantum yields, radiative lifetimes, and collisional rate coefficients with Ne, Ar, and N_2 were determined.

DD FORM
1 JAN 73 1473   EDITION OF 1 NOV 65 IS OBSOLETE   i

410 281

CONTENTS

79 09 14 076

INTRODUCTION

The first three years of this project were under the leadership of
Dr. S. A. Edelstein and were aimed primarily towards a physical
understanding of the partitioning of energy among the products of
elementary metathesis reactions of the type

$$A + BC \rightarrow AB + C$$

and the mechanisms by which that energy is transferred. The experi-
mental approach was one of emission spectroscopy combined with laser-
induced fluorescence to monitor populations in the various levels. The
studies were highly successful. The publications that have resulted
from this work have been described in three previous Interim Scientific
Reports.

With the departure of Dr. Edelstein, the Principal Investigator was
transferred to Dr. G. Black and Dr. D. Lorents although the general
scientific goals did not change. The experimental approach was
expanded to include the generation of electronically excited states
of atoms and diatomic molecules by photodissociation of triatomic
molecules in the vacuum ultraviolet. Because there are no generally
available lasers that offer wide wavelength coverage in this wavelength
region, these experiments have used the vacuum ultraviolet emission of
both a hydrogen lamp and synchrotron radiation, in conjunction with
monochromators, as photolytic sources. Emission spectroscopy continued
to be used to monitor the generation and decay of excited species.

One diagnostic of energy transfer mechanisms involves the effect
of temperature on reaction rate. In such studies, the temperature
range is often restricted by a number of experimental considerations.

1

When extending gas phase measurements to low temperature, one is ultimately limited by the vapor pressure of the source molecule (when using photodissociation as the production technique). By dissolving the source molecules in liquid rare gases (and nitrogen), we remove this problem (and several other restrictions) and have been able to extend our studies of energy transfer mechanisms down to $77^{o}K$ -- the temperature of liquid nitrogen. We have found that such high density media do not inhibit photodissociation and provide a unique opportunity to study energy transfer reactions at low temperature.

For studying the kinetic properties of short-lived species generated by photodissociation, the light source must be pulsed and have a decay time shorter than (or at least comparable to) the lifetimes of the species under study. The synchrotron radiation available at the Stanford Synchrotron Research Laboratory has a pulse duration of 0.3 nsec and repeats at 1.28 MHz. We have used this light source to study energy transfer reactions of the various electronically excited states of XeF with lifetimes in the 1-100 nsec range where the XeF^{*} was generated by photodissociation of XeF_2. Further support for these XeF^{*} experiments has been provided by the Defense Advanced Research Projects Agency under Contract DASG60-77-C-0028 through the U. S. Army BMDATC.

2

SUMMARY OF RESEARCH FINDINGS

The earlier successes in the research performed under Dr. Edelstein between June 1975 and July 1978 have been fully described in previous Interim Scientific Reports and will not be discussed further. A list of publications generated on this contract is given in Appendix A. The work performed during the past year has involved two distinct topics. The first of these was the production and properties of $O(^1S)$ and $S(^1S)$ at low temperatures in liquid argon and nitrogen. The second was the properties of the XeF (B and C) states under more conventional gas phase conditions. Brief descriptions of each of these topics follow.

Production and Properties of $O(^1S)$ at Low Temperature

$O(^1S)$ was produced by photodissociation of N_2O in liquid argon and nitrogen, and spectra of the resulting emissions were obtained. The quantum yield for its production was found to be similar to that previously measured[1] in the gas phase (for 144 to 147 nm). In both liquids, the resulting emission had a radiative lifetime of (13 ± 1) μsec. Studies of the quenching of $O(^1S)$ by N_2O in these liquids and in the gas phase over the temperature range 298-120 K suggested that an impurity in the N_2O became the dominant quencher at low temperature. This most extensive study of the temperature coefficient for $O(^1S)$ quenching by N_2O gave a rate coefficient of $7.0 \times 10^{-11} \exp(-1250/RT)$ cm^3 $molec^{-1}$ sec^{-1} (± 10%) over the temperature range 370 to 200 K. A fuller description of these measurements and their implications can be found in Appendix B of this report.

---

[1] G. Black, R. L. Sharpless, T. G. Slanger, and D. C. Lorents, J. Chem. Phys. 62, 4266 (1975).

3

Production and Properties of S(^{1}S) at Low Temperature

Photodissociation of OCS between 144 and 161 nm was used to produce S(^{1}S) in both liquid argon and nitrogen. Spectra of the resulting emissions were recorded. Over this wavelength range, the quantum yields were found to be within a factor of two of those previously measured[2] in the gas phase. The resulting emission had a radiative lifetime of (39 ± 2) μsec in liquid argon and (50 ± 3) μsec in liquid nitrogen. From the dependence of the emission decay time on OCS concentration, a rate coefficient of (4 ± 1) x 10^{-14} cm^3 $molec^{-1}$ sec^{-1} was found for the quenching of S(^{1}S) by OCS in both liquids. Further details and a discussion of the nature of S(^{1}S) in these media can be found in Appendix C.

XeF$_2$ Photodissociation Studies

Photodissociation of XeF$_2$ with synchrotron light pulses (0.3-nsec duration) was used as the source of XeF (B, C, and D) states. Intensity-time profiles were recorded using a photomultiplier-time-to-amplitude-converter system, which enabled decays as short as 1 nsec to be measured. Most of the measurements were made in the strong absorption band between 145 and 175 nm. At the peak of this band (158 nm), an absorption cross section of (6.0 ± 0.6) x 10^{-17} cm^2 was determined. By comparison with O(^{1}S) signals from N_2O, quantum yields for B, C, and D state production were determined. The decay time measurements gave radiative lifetimes of (13 ± 1) and (100 ± 10) nsec for the B and C states, respectively, as well as rate coefficients for a number of processes with Ne, Ar, and N_2. This work is more fully described in Appendix D.

Appendices B, C, and D are being prepared for publication in the Journal of Chemical Physics.

---

[2] G. Black, R. L. Sharpless, T. G. Slanger, and D. C. Lorents, J. Chem. Phys. 62, 4274 (1975).

Appendix A

PUBLICATIONS SUPPORTED BY THIS CONTRACT

1. "Chemiluminescence from Three-Body Reactions in the Ba + O_2 Flame," by S. A. Edelstein, B. E. Perry, D. J. Eckstrom, and T. F. Gallagher, Chem. Phys. Lett. <u>49</u>, 293 (1977).

2. "BaO($X^1\Sigma^+$) Vibrational Relaxation," by S. A. Edelstein, B. E. Perry, D. J. Eckstrom, and T. F. Gallagher, Chem. Phys. Lett. <u>50</u>, 271 (1977).

3. "Intermultiplet Energy Transfer in BaCl($C^2\Pi$)," by S. A. Edelstein, B. E. Perry, and T. F. Gallagher, Chem. Phys. Lett. <u>51</u>, 552 (1977).

4. "Intermultiplet Energy Transfer in BaCl($C^2\Pi$)," by S. A. Edelstein, D. L. Huestis, and J. Wyss, J. Chem. Phys. <u>70</u>, 131 (1979).

5. "Collisional Quenching of BaCl($C^2\Pi$) by He, Ar, and N_2," by S. A. Edelstein, J. Chem. Phys. <u>70</u>, 591 (1979).

6. "Resonance Ionization Velocimeter," by S. A. Edelstein and W. E. Cooke, submitted to J. Appl. Phys.

7. "Production and Properties of $O(^1S)$ in Liquid Argon (88°K) and Nitrogen (77°K)," by G. Black, R. L. Sharpless, and D. C. Lorents, to be submitted to J. Chem. Phys.

8. "Production and Properties of $S(^1S)$ in Liquid Argon (88°K) and Nitrogen (77°K)," by G. Black, R. L. Sharpless, and D. C. Lorents, to be submitted to J. Chem. Phys.

9. "XeF_2 Photodissociation Studies. I. Quantum Yields and Kinetics of XeF(B) and XeF(C)," by G. Black, R. L. Sharpless, D. C. Lorents, D. L. Huestis, R. Gutcheck, T. Bonifield, D. Helms, and G. K. Walters, to be submitted to J. Chem. Phys.

Appendix B

PRODUCTION AND PROPERTIES OF O(^{1}S) IN LIQUID ARGON (88°K) AND NITROGEN (77°K)

G. Black, R. L. Sharpless and D. C. Lorents
Molecular Physics Laboratory
SRI International, Menlo Park, California 94025

ABSTRACT

O(^{1}S) is produced by photodissociation of N_2O in liquid argon and liquid nitrogen with an efficiency similar to that previously measured in the gas phase (for 144-147 nm). Spectra of the resulting emissions have been recorded. In both liquids, the emissions have a radiative lifetime of (13 ± 1) μsec. Studies of the quenching of O(^{1}S) by N_2O in these liquids and in the gas phase over the temperature range 298-120°K suggest that an impurity in the N_2O becomes the dominant quencher at low temperatures. It is suggested that the gas phase quenching of O(^{1}S) by N_2O is best represented by $7.0 \times 10^{-11} \exp(-1250/RT)$ cm^3 molec^{-1} sec^{-1} with an estimated uncertainty of $\pm 10\%$ over the temperature range 370 to 200°K.

MP79-55

INTRODUCTION

Over the last ten years considerable progress has been made in understanding the production and removal processes of $O(^1S)$ in gas phase systems. Motivation for much of the early work came from the prominence of the 557.7 nm emission of $O(^1S)$ in the airglow and auroral emissions originating in the earth's upper atmosphere. This emission provides an in situ probe of the chemical state of the upper atmosphere if the production and removal processes are understood. During the last five years, further impetus for studies of $O(^1S)$ has been provided by the search for high energy laser amplifier devices suitable for laser fusion. For such an application the ^1S states of O, S and Se have many desirable characteristics.[1] Research in this area has concentrated on photolytic mechanisms for producing these excited states and the processes which remove them--mainly photoionization, quenching and collision-induced emission.

In addition to these extensive gas phase studies, $O(^1S)$ has also been studied in solid hosts at very low temperatures ($\sim 10^{\circ}K$). This work dates back over fifty years to the pioneering work of Vegard[2] and McLennan.[3] In this area of matrix spectroscopy a considerable increase in activity has occurred in recent years.[4-7]

Surprisingly, the properties of $O(^1S)$ in low temperature liquified rare gases have received little attention. The only previous work in

this area are studies carried out in this laboratory[8] using e-beam
excitation. The present work extends upon these earlier studies It
utilizes photolytic production of $O(^1S)$ (from N_2O) in both liquid argon
and liquid nitrogen. The decay times measured are related to the
radiative properties of $ArO(2^1\Sigma^+)$. The rate coefficients for quenching
the emission by N_2O have been measured in both liquid argon ($88^\circ K$) and
liquid nitrogen ($77^\circ K$). In order to understand the unexpectedly high
rate coefficients obtained at these low temperatures we have measured the
rate coefficient for quenching $O(^1S)$ by N_2O in the gas phase from $296^\circ K$
down to $120^\circ K$.

EXPERIMENTAL

The major part of the apparatus has been described in detail

elsewhere.[9] In summary, radiation from a low-pressure capillary discharge

in hydrogen, pulsed at 380 Hz, is dispersed by a 1-m monochromator (a

bandpass of 1.6 nm was used in most experiments), enters a 30 cm long

chamber and impinges on a sodium salicylate-coated Pyrex disc, which is

viewed from behind by an EMI 9514S photomultiplier. For these measurements,

the chamber was modified to incorporate a dewar system to contain the

liquified rare gases as shown in Figure 1. The cell was constructed of

OHFC copper with an internal volume of $\sim 15\, cm^3$. It had four windows of

3/4" diameter UV grade sapphire sealed with indium O-rings. The cell was

positioned so that two of these windows allowed the photolysis beam to

enter and leave the copper cell. The other two windows on the cell were

at right angles to this axis and allowed any fluorescence excited in the

cell to be viewed with an appropriate filter-photomultiplier combination.

For these measurements an EMI 9558QAM photomultiplier was used in

conjunction with either a 560 nm interference filter (halfwidth 10 nm)

or a combination of a Corning 3-69 and a 600 nm short-pass filter. This

latter filter combination had a 76% transmission at 558 nm with a

bandpass (1% transmission figure) from 520 to 620 nm. Some initial

measurements with a Wratten #4 filter (transmitting $\lambda > 470$ nm) gave a

two component decay. Only the fast decay was observed through the other

filters. The nature of the slow component will be the subject of future

work. The photomultiplier was operated at -20°C giving a dark count of ~ 20 sec^{-1}. As in our previous gas phase experiments, the photomultiplier output was recorded as a function of time using a MCA.

The liquid sample cell was pumped by a gas handling system through 1/2" stainless steel thin wall tubing. An additional pump port is located at the bottom of the cell to provide for cell cleaning by circulating clean gas through the cell. The cell was pumped down to the lower 10^{-6} torr range before liquification of a sample. The gas handling system contained a 30 liter volume in which N_2O/Ar and N_2O/N_2 mixtures were made up. Oxygen and water vapor were removed from the argon by passage over a heated Ti getter (850°C) while the nitrogen was purified by heated copper at 400°C (to remove oxygen). The initial argon and nitrogen used were > 99.995% pure. Liquid argon (88°K) was used to liquify and maintain the N_2O/Ar mixtures (and liquid N_2 for the N_2O/N_2 mixture) in order to avoid the problem of solidification of the argon samples that would occur with liquid nitrogen (the melting point of argon is 84°K). Transmission through the resulting liquids showed that the techniques employed reduced the O_2 concentration to $\ll 1$ ppm. The N_2O was added through a dry-ice/acetone trap.

N_2O was initially introduced to the 30 liter mixing volume at a pressure of 10^{-4} to 10^{-2} torr to provide a mixture containing 0.07-7 ppm after admission of up to two atmospheres of argon. Turbulence created by the argon addition was found to mix the contents of the 30 liter volume. This resulting mixture was allowed to expand into the cell before cooling

the cell and liquifying the sample with liquid argon or nitrogen. The center region traversed by the photolysis beam was completely filled with liquid.

In addition to these liquid phase experiments, we also made measurements in the gas phase at temperatures down to $\sim 125^{\circ}K$ using gas mixtures of 0.15-0.6 torr of N_2O in two atmospheres of argon (or nitrogen). For these measurements the cell was first cooled with liquid nitrogen to $\sim 125^{\circ}K$, the gas sample admitted and, after a few minutes to establish thermal equilibrium, the decay time of the emission was determined. The measurement was repeated at a number of temperatures as the cell warmed up.

In addition to these kinetic properties, the spectral nature of the emissions in both liquid argon and nitrogen were measured using an image intensified spectrograph.[10] The emissions produced by the wavelength-resolved light from the monochromator were too weak to record with this spectrograph so the spectra were produced by a microwave-powered H_2 lamp placed at the detector end of the evacuated photolysis cell. In order to reduce the interference by scattered visible light from the H_2 lamp, its output was filtered with a vacuum ultraviolet Acton filter having 36% transmission at 145 nm and a 60 nm bandwidth (50% peak transmission).

RESULTS AND DISCUSSION

The spectral nature of the $^1S - {}^1D$ emission, in both liquid argon and liquid nitrogen, are shown in Fig. 2. In each case a broad predominantly red degraded continuum band is produced. This differs from the predominantly blue degraded emission found in spectra of $O(^1S)$ in gas phase argon and nitrogen[11,12] and is difficult to explain in terms of expected diatomic interaction potentials. Our liquid phase spectra show striking similarity to the red-shifted emissions from $O(^1S)$ observed in argon matrices.[4,7] In both the published argon-matrix spectra[4,7] the strongest emission feature occurs close to, but slightly red-shifted (~ 2 nm) from the position of the unperturbed $O(^1S \rightarrow {}^1D)$ emission at 557.7 nm--Brom and Broida[4] find a sharp doublet at 559.0 ± 0.1 and 560.0 ± 0.1 nm whereas Taylor and Walker[7] find a single peak at 559 nm. In addition both papers report weaker emission appearing as a broad shoulder at longer wavelengths (≈ 565 nm). The spectra in Fig. 2 suggest that the same two features are present in liquid argon and nitrogen. In the solid phase the two features are thought to arise[7] because the $O(^1S)$ can occupy two different sites which can give rise to emissions at different wavelengths with different lifetimes. (Different lifetimes have been measured[6] for the two emission features in a krypton matrix but similar measurements in argon do not exist.) It seems likely that similar sites in the liquid will be present but subject to continuous destruction and reformation reflecting the

dynamic properties of the liquid state. This state of rapid equilibrium

between the two sites expected in the liquid state suggests that only one

lifetime should be observed in the liquid state. This is consistent with

our observation of only one decay time in liquid argon (and nitrogen).

A typical kinetic experiment is shown in Fig. 3 for $N_2O = 0.20 \times 10^{16}$ cm^{-3}

(i.e. 0.095 ppm in liquid argon). ·Very strong signals were obtained

despite strong absorption by the sapphire windows at the exciting wave-

length of 144 nm. The decay rate of the emission as a function of N_2O

is shown in Fig. 4. Fig. 4 also includes the measurements in liquid

nitrogen. If the changing decay rate is due to quenching by N_2O, the

slopes of the lines in Fig. 4 give 2.5×10^{-12} cm^3 $molec^{-1}$ sec^{-1} for

quenching of the emitting state by N_2O in liquid argon at $88^\circ K$ and

1.1×10^{-12} cm^3 $molec^{-1}$ sec^{-1} in liquid nitrogen at $77^\circ K$ with estimated

uncertainties of $\pm 10\%$. However it will be shown late that quenching

under this condition is likely controlled by impurities. For both

liquid argon and nitrogen the intercepts give (13 ± 1) μsec for the lifetime

in the absence of N_2O quenching. The interaction between argon and $O(^1S)$

has been shown to involve only a radiative (collision-induced emission)

path[13] between 291 and $201^\circ K$. If this holds at $88^\circ K$, then 13 μsec is

the radiative lifetime of $O(^1S)$ in liquid argon. We also see a considerable

lengthening of the emission lifetime when we solidify our liquid argon

solutions by cooling to liquid nitrogen temperatures and below. At

liquid N_2 temperature (77°K) we measured (32 ± 1) μsec increasing to

(35 ± 1) μsec at 67°K (the lowest temperature obtained) with N_2O =

0.18×10^{16} cm^{-3}. A more detailed discussion of these various properties

of the emission follows.

I   Quantum Yield for $O(^1S)$ Production

From the intensity of the signals obtained we can estimate the

efficiency of $O(^1S)$ production from N_2O in liquid argon. The necessary

measurements, for a wavelength of 144 nm, are shown in Fig. 5. They were

made using the combination of the Corning 3-69 and 600 nm short-pass

filter. Decays of the emission produced in both liquid argon at 88°K

and gaseous argon (1320 torr) at 153°K are shown. We used cooled, rather

than room temperature, argon because the transmission of the sapphire

windows at 144 nm was greatly increased by cooling to 153°K. Little

further change in transmission was observed by cooling to the 88°K

temperature of liquid argon. The two experiments were conducted with

approximately the same photolysis beam intensities and N_2O concentrations

which, within the experimental uncertainty ($\pm$ 20%), provided the same

absorption rate of photons in both the gas and liquid samples. Extrapolating

the lines in Fig. 4 to -15 μsec [the time the H_2 lamp producing the $O(^1S)$

was pulsed] gives a ratio of initial intensities of 260. Assuming that

the quantum yields for $O(^1S)$ production are the same, this ratio should

equal the ratio of radiative lifetimes (assuming the same fraction of the

B-9

emission is being seen in each case). For the gas phase experiment we do not have a measure of the rate coefficient for collision-induced emission at $153^\circ K$ but, based on Welge's observation[13] of no change from 291 to $201^\circ K$, we have assumed no temperature dependence and used the room temperature value. This gives 389 sec^{-1} for the collision-induced radiative rate with 1320 torr of argon at $153^\circ K$. The ratio of the liquid radiative decay rate of 7.6×10^4 sec^{-1} to this gas phase value is 200 compared to 260 for the intensity ratio. Within the limits of these assumptions, it appears that photodissociation of N_2O in liquid argon at 144 nm produces $O(^1S)$ with a quantum yield similar to that measured in the gas phase.[9,14] A similar conclusion also applies to the measurements in liquid nitrogen. We must also conclude that 13 μsec is the radiative lifetime and that any quenching must play a minor role. In contrast to the similarity of yields in the liquid and gas phases, Brom's results[4] for N_2O in a solid argon matrix at $4^\circ K$ seem to indicate that the ratio of $O(^1S)$ to $N(^2D)$ production is higher than in the gas phase (at 121.6 nm) implying either a higher ^1S quantum yield or a lower $N(^2D)$ quantum yield (or both) in the solid phase. These measurements, however, were not conclusive and further work would be required to determine the quantum yields in the solid phase.

II   Radiative Lifetime of ArO($2\,^1\Sigma^+$)

Having determined the emission spectrum and the radiative lifetime

for O(^{1}S) in liquid argon, we discuss the nature of O(^{1}S) in this

medium--in particular, the fraction of the O(^{1}S) which exists as bound

diatomic ArO($2\,^1\Sigma^+$) molecules. We attempt an estimate of the fraction

of the emission which is produced by these bound molecules compared to

that produced by collisions on the repulsive wall of the $2\,^1\Sigma^+$ potential

above the dissociation limit (referred to as the "free" emission of O(^{1}S)).

It is noteworthy that the emission shows substantial broadening in both

blue and red directions.

This essentially gas phase view of our liquid phase experiment

must of necessity be an approximate one. The very extent of the red

degraded emissions observed in both liquid and solid argon is much more

than can be expected from the binding in the ArO($2\,^1\Sigma^+$) potential. It is

clear that more complicated Ar-O interactions, involving several Ar

neighbors, will also contribute binding sites in both liquid and solid

phases. However, we do not have the ability to quantify the effects of

these more complicated interactions. It is therefore of interest to

apply gas phase considerations if only to show the limitations of such

an approach. Further insight is provided by comparison with results in

an argon matrix.[4,7]   The similarity of the spectra has already

received comment. However we observe that much longer lifetimes are

produced by freezing the argon. This must reflect the combination of

two effects--restricted molecular motion and the greater symmetry of the environment surrounding the $O(^1S)$ atom (remembering that it is essentially the cylindrical distortion produced by the approach of one argon atom which results in shortening the radiative lifetime).

One approach to determining the nature of $O(^1S)$ in liquid argon involves estimating the equilibrium constant for the process

$$O(^1S) + Ar + Ar \rightleftharpoons ArO(2^1\Sigma^+) + Ar \quad . \qquad (1)$$
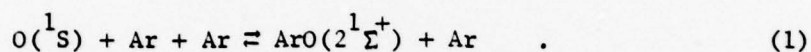
In general, the equilibrium constant involves products of translational and internal partition functions, Q

$$K = \left(\frac{h^2}{2\pi\mu kT}\right)^{3/2} \frac{Q_{ArO(2^1\Sigma^+)}}{Q_{Ar} \cdot Q_{O(^1S)}} \cdot e^{D/kT} \quad .$$

Estimates for D, the dissociation energy, range from 25 to 70 cm^{-1} (references 15, 17). We have used a value of 50 cm^{-1} based on the binding in the corresponding mixed rare gas (NeAr) ground state potential.[18] Using 3.13 Å for the $Ar-O(^1S)$ bond[15] and, for lack of knowledge, approximating the vibrational partition function by unity, we obtain $K = 1.5 \times 10^{-22}$ $cm^3 molec^{-1}$ at $88^\circ K$. For $Ar = 2.11 \times 10^{22}$ cm^{-3}, appropriate to liquid argon, this gives a ratio of $[ArO(2^1\Sigma^+)]/[O(^1S)] = 3.2$. This estimate is probably no better than an order of magnitude. Furthermore, evidence that a substantial fraction of the $O(^1S)$ is still unbound is provided by consideration of the rate coefficient for collision-induced emission by argon. Welge and Atkinson[13] found a value of $(4.8 \pm 0.5) \times 10^{-18}$ $cm^3 molec^{-1} sec^{-1}$ at $291^\circ K$ (confirmed by Black et al.[19]) and a similar

value at 201°K. At these temperatures the emission is mainly from
unbound atoms and the effective two-body emission coefficient for this
process only decreases very slowly with temperature.[17] Hence, applying
the same value at 88°K for the density of liquid argon would give a
radiative rate of $\sim 10^5$ sec^{-1} if the amount of $O(^1S)$ bound in ArO is
still a small fraction of the total $O(^1S)$ at 88°K in liquid argon. This
is sufficiently close to our measured value of 7.7×10^4 sec^{-1} to
indicate that a substantial amount of the $O(^1S)$ must still be unbound.
Furthermore, theoretical calculations[17] indicate that in the gas phase
at a temperature as low as 78°K, unbound atoms are still responsible
for a major part of the emission. It is clear, therefore, that one
cannot ignore the contribution of free $O(^1S)$ to the emission--particularly
because of the rapidly rising transition moment on the repulsive wall
of the $ArO(2^1\Sigma^+)$ potential.[16-18] We must conclude, therefore, that
because of the unknown contribution of bound ArO to the measured 13 μsec
lifetime we are unable to extract a value for the radiative lifetime of
bound $ArO(2^1\Sigma^+)$, τ_R.

There are a number of estimates of τ_R available in the literature.
From studies of collision-induced emission and estimates of the
equilibrium constant, values of 4 μsec and 7 μsec have been estimated
at room temperature[12,13] and 8 μsec at 201°K.[13] From measurements of
laser gain,[20] a value of $\sim$ 10 μsec has been deduced for the radiative
lifetime of bound $ArO(2^1\Sigma^+)$.

We can also compare our measured lifetime with the lifetimes

calculated by Dunning and Hay.[16] These calculations apply to the free

emission from the repulsive wall of the potential for which they give

the formula

$$A_p = \tau_p^{-1} = 1.063 \times 10^6 \; g_i \; \mu_{ij}^2 \; \Delta E^3 \; sec^{-1}$$

where μ_{ij} is given in atomic units, ΔE is in eV and g_i is the degeneracy

factor. This results in 23 μsec for the radiative lifetime of the free

ArO $2^1\Sigma^+ - 1^1\Sigma^+$ transition[16] at 298°K and 47 μsec at 88°K. The latter

number is difficult to reconcile with our measured value of 13 μsec or

the various estimates of τ_R. The discrepancy must arise, at least in

part, from the neglect of emission from bound molecules, which although

at larger internuclear separation and hence smaller transition moment,

have the compensating feature of longer time at that distance.

We must also consider the possibility that the argon-oxygen distance

is shortened by the effect of the liquid argon matrix. However, in view

of the Ar-Ar distance of 3.6 Å compared to an estimated Ar-O distance of

3.13 Å, this effect is not expected. In previous work on e-beam pumped

liquid argon-oxygen mixtures[8] the intercept at zero oxygen addition

was 7 μsec. This shorter lifetime is now thought to be due to the

generation of small amounts of O_3 during that experiment and subsequent

fast-quenching of $O(^1S)$.[21] At the present time, therefore, it appears

that insufficient information is available to interpret the 13 μsec

radiative lifetime observed. It is also interesting to compare the 13 μsec lifetime in liquid N_2 at 77°K with the ≈ 200 μsec lifetime observed[22] in solid nitrogen at 4°K where the effects of restricted molecular motions and higher symmetry in the environment become most apparent.

III Quenching of $O(^1S)$

In liquid argon and nitrogen, the decay rate of the emissions vs N_2O (Figure 3) gives quenching rate coefficients much higher than expected based on a previous study[23] of $O(^1S)$ quenching by N_2O over the temperature range 350-200°K. Extrapolation of this gas phase study to the temperatures of 88°K and 77°K gives rate coefficients almost an order of magnitude smaller than observed. A possible explanation for this difference involves quenching of bound $ArO(2^1\Sigma^+)$ molecules by N_2O. It is also possible, however, that impurities in the N_2O, quenching $O(^1S)$ with high efficiency, dominate the quenching at low temperature. To check this possibility the previous gas phase measurements were extended down to $\sim 120^\circ$K (limited by the N_2O vapor pressure). An Arrhenius plot of the quenching rate coefficients vs 1/T is shown in Figure 6. Curvature in this plot is apparent and the gas phase values at the lowest temperature are the same as the value in liquid argon. Since the gas phase experiments (at $\sim$ 1500 torr argon or nitrogen) would have little bound $O(^1S)$ present, another explanation must be found. The most

B-15

reasonable hypothesis is that an impurity is responsible for both the curvature in the Arrhenius plot and the unexpectedly high quenching rate in liquid argon (and nitrogen). The lower value in liquid N_2 may reflect a change in the nature (perhaps arising from association) of the quenching impurity in this medium. The prime suspect for the impurity is water vapor that is not being removed by the dry ice/acetone trap. The problem of impurities in N_2O effecting quenching rate coefficients is a long standing one--early measurements[24,25] of $O(^1S)$ quenching by N_2O gave values of 1.5×10^{-11} $cm^3 molec^{-1} sec^{-1}$ and 1.6×10^{-11} $cm^3 molec^{-1} sec^{-1}$, later values in these same two laboratories[26,27] were 1.1×10^{-11} $cm^3 molec^{-1} sec^{-1}$ and 1.0×10^{-11} $cm^3 molec^{-1} sec^{-1}$ with the most recent value[9] $(8.7 \pm 0.9) \times 10^{-12}$ $cm^3 molec^{-1} sec^{-1}$. The new results suggest that the previous temperature dependent rate for N_2O quenching of $O(^1S)$ be replaced by $7.0 \times 10^{-11} \exp(-1250/RT)$ $cm^3 molec^{-1} sec^{-1}$ with an estimated uncertainty of $\pm 10\%$ for $370-200\,^{\circ}K$.

Conclusions

We have shown, assuming no temperature dependence to collision-induced emission between 201 and $153\,^{\circ}K$, that the photodissociation of N_2O to give $O(^1S)$ in the 144-147 nm range in liquid argon and nitrogen has a similar quantum yield to that previously measured in the gas phase. Weighing all the evidence, it appears that the 13 μsec radiative lifetime of the resulting emission contains contributions from both bound and free $O(^1S)$ with the individual contributions as yet undetermined.

The emission spectra of $O(^1S)$ in liquid Ar and N_2 support this conclusion. We have demonstrated that an impurity in N_2O (probably water vapor) became the dominant $O(^1S)$ quencher at low temperatures and that the gas phase quenching of $O(^1S)$ by N_2O is best represented by $7.0 \times 10^{-11} \exp(-1250/RT)$ cm^{3}molec^{-1}sec^{-1} with an estimated uncertainty of $\pm$ 10% over the temperature range 370 to 200°K.

Acknowledgments

REFERENCES

1. J. R. Murray and C. K. Rhodes, J. Appl. Phys. $\underline{47}$, 5041 (1976).

2. Vegard published a large number of articles on his studies. Some of his more complete publications are: L. Vegard, Compt. Rend. 180, 1084 (1925); Ann. Physik $\underline{79}$, 377 (1926); Leiden Comm. $\underline{16}$, No. 175 (1924-1926); Leiden Comm. $\underline{19}$, No. 205 (1929-1931); Skrifter Norske Videnskaps-Akad. Oslo, No. 2 (1930).

3. J. C. McLennan and G. M. Shrum, Proc. Roy. Soc. (London) $\underline{A106}$, 138 (1924); J. C. McLennan, H. J. C. Ireton, and K. Thompson, Nature $\underline{118}$, 408 (1926).

4. J. M. Brom, Jr., and H. P. Broida, Chem. Phys. Lett. $\underline{33}$, 51 (1975).

5. J. Goodman, J. C. Tully, V. E. Bondybey, and L. E. Brus, J. Chem. Phys. $\underline{66}$, 4802 (1977).

6. K. M. Monahan and V. Rehn, J. Chem. Phys. $\underline{68}$, 3814 (1978).

7. R. V. Taylor and W. C. Walker, J. Chem. Phys. $\underline{70}$, 284 (1979).

8. J. A. Margevicius, M. V. McCusker, L. Abouaf, D. C. Lorents, and D. L. Huestis,"Optical Emissions from Doped Condensed Rare Gases Excited by Electrons," presented at the 30th Gaseous Electronics Conference, Palo Alto, California, 18-21 October 1977; "ArS, XeO and ArO Emissions from Liquid Argon Hosts: Spectra and Kinetics," presented at the 10th International Quantum Electronics Conference, Atlanta, Georgia, 29 May-1 June 1978.

9. G. Black, R. L. Sharpless, T. G. Slanger, and D. C. Lorents, J. Chem. Phys. $\underline{62}$, 4266 (1975).

10. R. L. Sharpless and R. A. Young, Rev. Sci. Instrum. 41, 1628 (1970).

11. C. D. Cooper and M. Lichtenstein, Phys. Rev. 109, 2026 (1958).

12. D. L. Cunningham and K. C. Clark, J. Chem. Phys. 61, 1118 (1974).

13. K. H. Welge and R. Atkinson, J. Chem. Phys. 64, 531 (1976).

14. M. J. McEwan, G. M. Lawrence, and H. M. Poland, J. Chem. Phys. 61, 2157 (1974).

15. E. C Zipf, Bull. Am. Phys. Soc. 14, 265 (1969).

16. T. H. Dunning, Jr., and P. J. Hay, J. Chem. Phys. 66, 3767 (1977).

17. P. S. Julienne, M. Krauss, and W. Stevens, Chem. Phys. Lett. 38, 374 (1976).

18. P. S. Julienne, J. Chem. Phys. 68, 32 (1978).

19. G. Black, R. L. Sharpless, and T. G. Slanger, J. Chem. Phys. 63, 4546 (1975).

20. W. M. Hughes, N. T. Olson, and R. Hunter, Appl. Phys. Lett. 28, 81 (1976).

21. G. London, R. Gilpin, H. I. Schiff, and K. H. Welge, J. Chem. Phys. 54, 4512 (1971).

22. E. M. Hörl, J. Molec. Spectrosc. 3, 425 (1959).

23. T. G. Slanger and G. Black, J. Chem. Phys. 65, 2025 (1976).

24. F. Stuhl and K. H. Welge, Can. J. Chem. 47, 1870 (1969).

25. G. Black, T. G. Slanger, G. A. St. John, and R. A. Young, Can. J. Chem. 47, 1872 (1969).

26. S. V. Filseth, F. Stuhl, and K. H. Welge, J. Chem. Phys. 52, 239 (1970).

27. T. G. Slanger, B. J. Wood, and G. Black, Chem. Phys. Lett. 17, 401 (1972).

FIGURE CAPTIONS

Figure 1   Schematic diagram of cell for wavelength-resolved photolytic
excitation of doped liquid Ar or N_2 in the vacuum ultraviolet.

Figure 2   Emission following the production of $O(^1S)$, from N_2O photo-
dissociation in the wavelength region 140-150 nm, in both
liquid argon ($88^\circ K$) and nitrogen ($77^\circ K$). N_2O = 0.9 ppm.
Asterisks indicate scattered light from the H_2 photolysis
lamp.

Figure 3   Decay of $O(^1S)$ in liquid argon ($88^\circ K$) containing $[N_2O]$ =
0.20×10^{16} cm^{-3}. 30 min. experiment at λ = 144 nm.

Figure 4   Decay rate of $O(^1S)$ vs $[N_2O]$ in liquid argon ($88^\circ K$) and
liquid N_2 ($77^\circ K$).

Figure 5   Decay of $O(^1S)$ in both liquid and gaseous argon. In the
liquid argon ($88^\circ K$) experiment, $[N_2O]$ = 1.06×10^{16} cm^{-3} and
t = 10 mins. In the gas phase experiment (Ar = 1320 torr at
$153^\circ K$), $[N_2O]$ = 1.10×10^{16} cm^{-3} and t = 5 mins.

Figure 6   Arrhenius plot for $O(^1S)$ quenching by N_2O in the gas phase
using both N_2 (o) and Ar (●) at ≈ 1500 torr as buffer gases.
The rate coefficients measured in liquid argon ($88^\circ K$) and
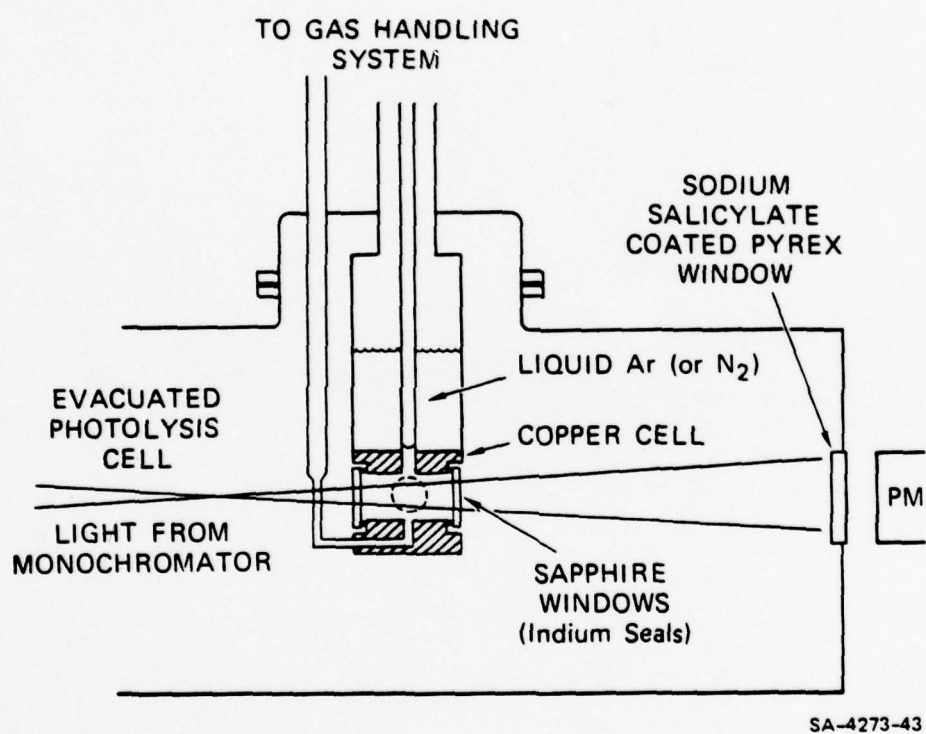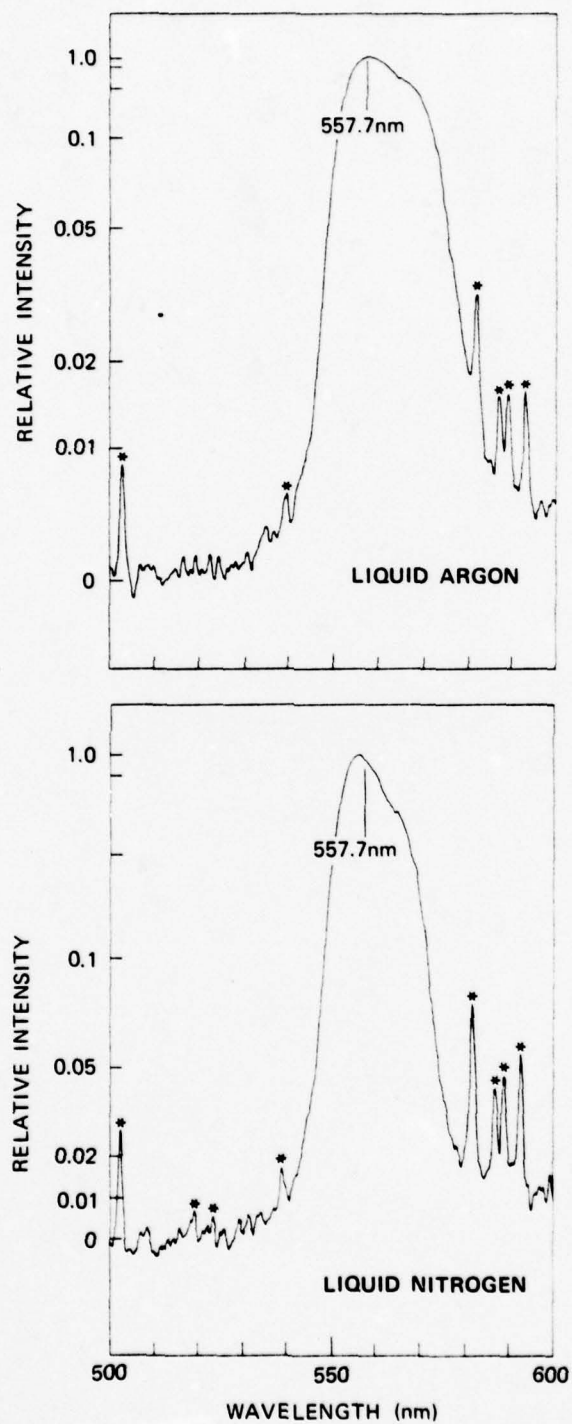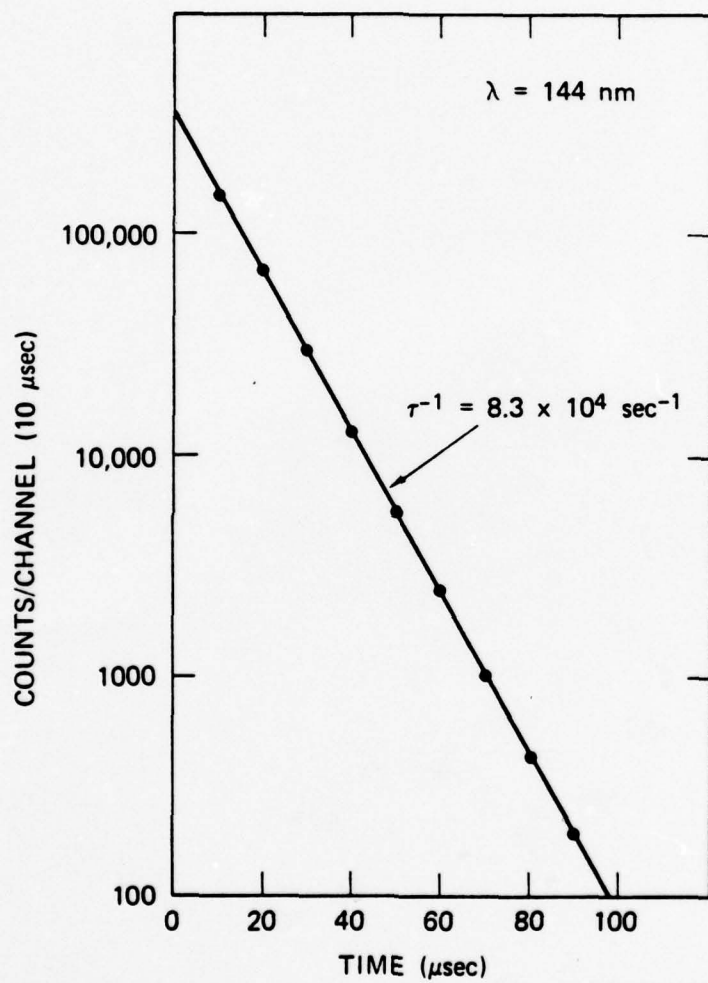liquid N_2 ($77^\circ K$) are also shown.

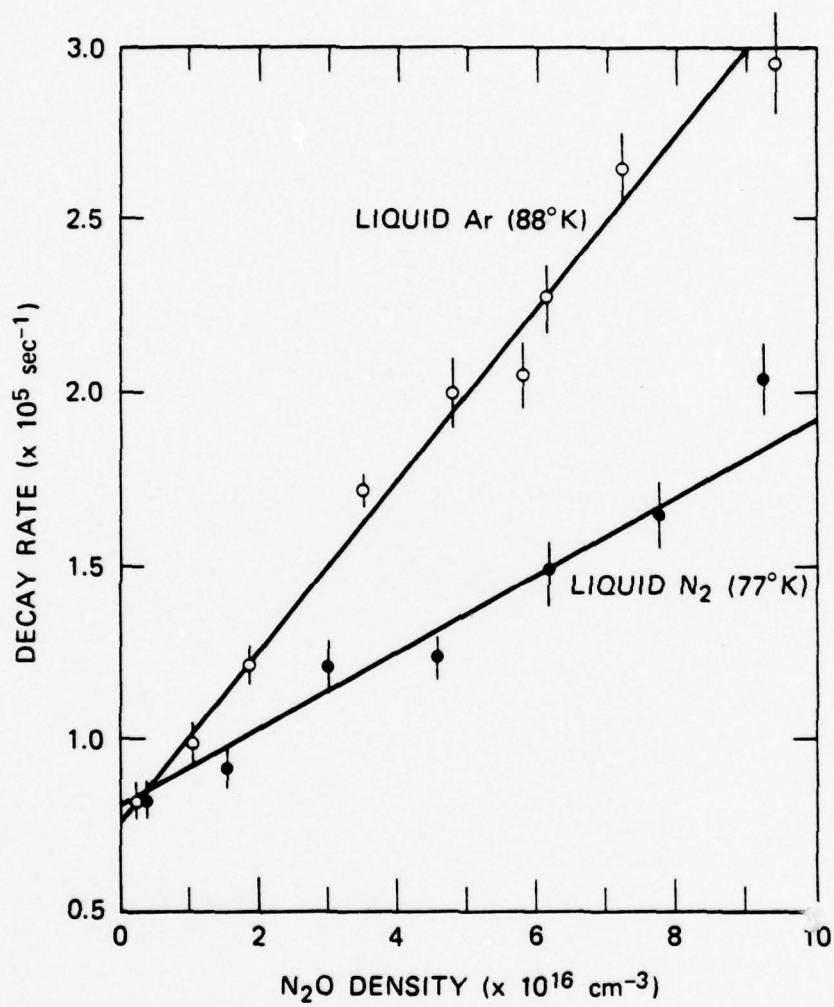TO GAS HANDLING SYSTEM

SODIUM SALICYLATE COATED PYREX WINDOW

EVACUATED PHOTOLYSIS CELL

LIQUID Ar (or N_2)

COPPER CELL

LIGHT FROM MONOCHROMATOR

SAPPHIRE WINDOWS (Indium Seals)

PM

SA-4273-43

Figure 1

B-21

Figure 2

λ = 144 nm

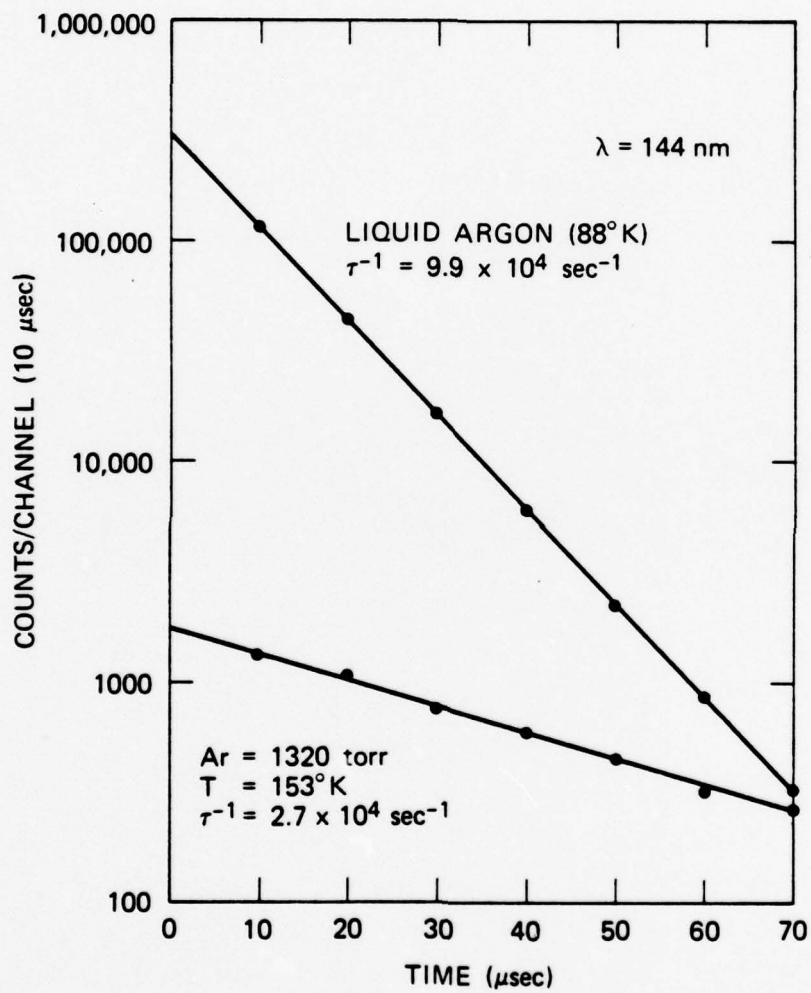τ^{-1} = 8.3 × 10^4 sec^{-1}
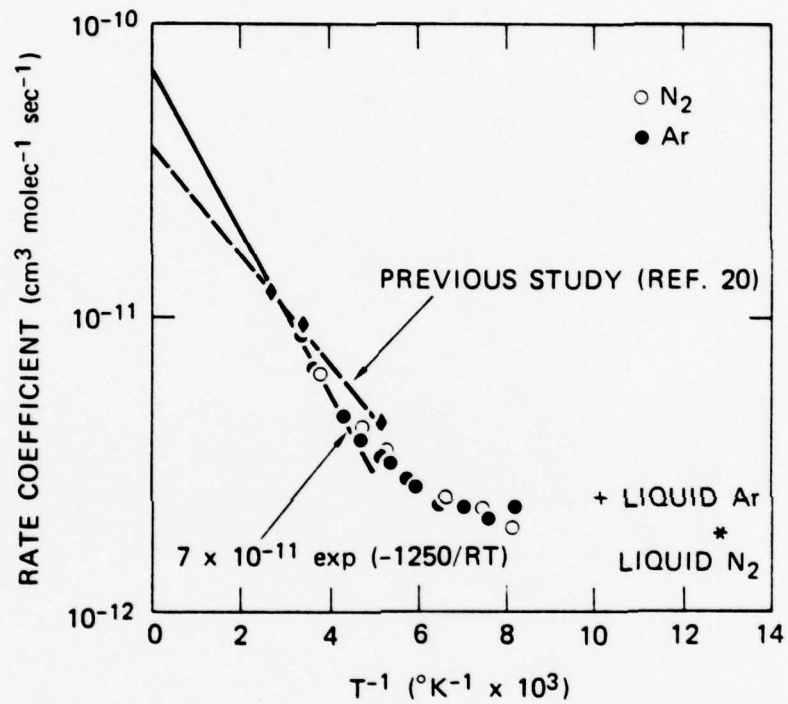
SA–4273–44

Figure 3

SA-4273-48

Figure 4

Figure 5

SA-4273-45

B-25

Figure 6

SA-4273-49

Appendix C

PRODUCTION AND PROPERTIES OF S(^{1}S) IN
LIQUID ARGON (88°K) AND NITROGEN (77°K)

G. Black, R. L. Sharpless, and D. C. Lorents
Molecular Physics Laboratory, SRI International
Menlo Park, California 94025

ABSTRACT

Photodissociation of OCS to produce S(^{1}S) has been observed in both liquid argon and liquid nitrogen over the wavelength range 144 to 161 nm. Over this wavelength range, the quantum yields are within a factor of two of those previously measured in the gas phase. Spectra of the emissions have been measured. The emissions have radiative lifetimes of (39 ± 2) μsec in liquid argon and (50 ± 3) μsec in liquid nitrogen. Evidence is presented that S(^{1}S) exists mainly as bound molecules in these media and that the lifetimes measured are those for the bound $2^1\Sigma^+ - 1^1\Sigma^+$ transitions. In these media the quenching of the emission by OCS has a rate coefficient of $(4 \pm 1) \times 10^{-14}$ cm^3 molec^{-1} sec^{-1}.

INTRODUCTION

Motivated by the laser fusion program, much work has been done on the photolytic production and properties of the ^1S states of O,S and Se. In the case of $S(^1S)$, efficient production from OCS was demonstrated[1] from 142 to 160 nm - a range which encompasses both the Kr_2 emission at 147 nm and the F_2 emission at 158 nm as potential photolytic sources in a high power laser amplifier. The collision-induced emission of $S(^1S)$ has been studied in this laboratory[2-4] and the quenching of $S(^1S)$ has been the subject of several earlier studies.[5-7] All this work has been confined to the gas phase.

Work in the solid phase has been confined to two studies[8,9] in which production of $S(^1S)$ was demonstrated at 147 nm by observation of its matrix-induced emission. No lifetime information was obtained. In this laboratory studies of OCS is liquid argon under both e-beam and H_2 laser (161 nm) irradiation[10] showed $S(^1S)$ production. With the H_2 laser, the radiative lifetime of $S(^1S)$ in liquid argon was measured as (35 ± 10) µsec. For the e-beam pumping experiment, (58 ± 9) µsec was obtained. Furthermore, a value of $(3.5 \pm 0.9) \times 10^{-13} cm^3 molec^{-1} sec^{-1}$ was obtained for the quenching of $S(^1S)$ by OCS in liquid argon. We have continued to study photolytic production and properties of $S(^1S)$ in liquid argon using wavelengths from 144 to 161 nm. The results are a substantial improvement on those obtained earlier.

EXPERIMENTAL

The apparatus and techniques are as described previously.[11] In addition to the Ar and N_2 used previously, the OCS was used as a 10.8% mixture in prepurified argon. It was added to the system through a dry ice/acetone trap. Mixtures with argon and nitrogen were made up in a 30 liter volume in which turbulence introduced by the addition of the major gas was used to mix the contents. Mixtures containing from 0.1 - 2 ppm of OCS in two atmospheres of argon or nitrogen were liquified as previously.[11]

For these experiments, a Wratten 89B filter - EMI 9558QAM photo-multiplier was used to view the emission in the vicinity of the ^1S - ^1D transition at 772.7 nm. The intensity-time profiles, following pulsed excitation, were recorded with a MCA as described previously.[11]

RESULTS AND DISCUSSION

The spectral nature of the emissions, in both liquid argon and liquid nitrogen, are shown in Fig. 1. As with $O(^1S)$ in these same media,[11] the $^1S_0 \rightarrow {}^1D_2$ atomic transition (at 772.7 nm) appears as a predominantly red degraded band which differs from the predominantly blue degraded emission found in the gas phase.[3] We also see emission in the vicinity of the atomic transition at 459 nm $[{}^1S_0 \rightarrow {}^3P_1]$ in both liquids with approximately 0.005 the intensity of the long wavelength transition. No structure is apparent in the 459 nm feature. It does, however, exhibit a blue shift in liquid nitrogen (as does the long wavelength transition) relative to the position of the atomic line. No such shift is seen in liquid argon.

Measurements of the $S(^1S)$ emission decay were made over the wavelength range 144 to 161 nm. A typical decay, using 158 nm excitation and liquid N_2 at $77^\circ K$ as the solvent is shown in Fig. 2. The decay rates versus OCS concentration, for measurements in both liquid argon and nitrogen, are shown in Fig. 3.

Measurements of relative quantum yields for $S(^1S)$ production over the range 144 to 161 nm, made in a similar way to the previous gas phase measurements,[1] established that the relative quantum yield versus wavelength curve had a similar shape to that measured in the gas phase. Furthermore, comparison with gas phase signals at 161 nm established that the absolute yields were within a factor of two of those measured

in the gas phase. It appears, therefore, that these dense media do not substantially effect the photolytic yield of $S(^1S)$ atoms.

The intercepts of Fig. 2 give (39 ± 2) μsec for the radiative lifetime of $S(^1S)$ in liquid argon and (50 ± 3) μsec for the radiative lifetime of $S(^1S)$ in liquid nitrogen. The former value is in agreement with, but considerably more precise than the (35 ± 10) μsec obtained previously[10] in this laboratory for H_2 laser (161 nm) excitation but considerably smaller than the (58 ± 9) μsec obtained with e-beam excitation. Both the previous measurements were affected by rapid depletion of the OCS and by long-lived emission of $S_2(B{\rightarrow}X)$ radiation thought to arise from sulfur atom recombination.

As in our previous study[11] of $O(^1S)$ in liquid argon, we require additional information to resolve the measured lifetime into components arising for bound $(2^1\Sigma^+)$ molecules and from free $S(^1S)$ atoms (which produce emission from the repulsive wall of the $2^1\Sigma^+$ potential up to $\sim kT$ above the dissociation limit). Some guidance is provided by consideration of the values of the rate coefficient for collision-induced emission by argon at 296 and 232°K determined in our previous work.[4] The values obtained were $(4.2 \pm 0.3) \times 10^{-18}$ and $(4.8 \pm 0.3) \times 10^{-18}$ cm^3 $molec^{-1}$ sec^{-1} at 296 and 232°K respectively, with the slight increase at the lowest temperature arising from bound emission. With further cooling, based on consideration of the analogous $O(^1S)$ - Ar system,[12] it is expected that the contribution from free emission will

fall slowly but will be more than compensated by the increasing contribution from bound molecules. Hence a value of 5×10^{-18} cm^3 $molec^{-1}$ sec^{-1} is expected to be a lower input on the collision-induced emission rate coefficient at $88°K$ (the temperature of liquid argon). Using this value, then a radiative lifetime of ≈ 10 μsec can be calculated for liquid argon density ($2.11 \times 10^{22} cm^{-3}$). This is sufficiently smaller than our measured value that a major fraction of the $S(^1S)$ must be bound in ArS molecules under these conditions.

A similar conclusion is reached by estimating the equilibrium coefficient for the process

$$S(^1S) + Ar + Ar \stackrel{K}{\rightleftharpoons} ArS(2^1\Sigma^+) + Ar$$
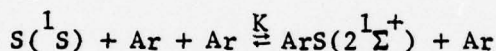
for which

$$K = \left(\frac{h^2}{2\pi\mu kT}\right)^{\frac{3}{2}} \frac{Q_{ArS\,(2^1\Sigma^+)}}{Q_{Ar} \cdot Q_{S(^1S)}} e^{D/kT}$$

where Q represents the internal partition function and D is the dissociation of the $ArS(2^1\Sigma^+)$ potential. Using $D = 98$ cm^{-1} (by approximating ArS to the corresponding rare gas ground state, Ar-Ar in this case)[13], an internuclear separation of 3.7 Å, and equating the vibrational partition function to unity we obtain $K(at\ 88°K) = 3.8 \times 10^{-22}$ cm^3 $molec^{-1}$. This gives $ArS(2^1\Sigma^+)/S(^1S) = 8$ for $Ar = 2.11 \times 10^{22} cm^{-3}$. Although this is only an order of magnitude calculation, consistency with the above discussion of collision-induced emission reinforces the

conclusion that $S(^1S)$ in liquid argon exists mainly as bound $ArS(2\,^1\Sigma^+)$ molecules and that the radiative lifetime of $ArS(2\,^1\Sigma^+)$ is close to the measured value. A similar conclusion holds for the analogous molecule with N_2. As with our $O(^1S)$-liquid argon study,[11] we are unable to assess the effects of interacting with several neighboring argon atoms which must occur in the liquid medium.

The slopes of both lines in Fig. 2 give a rate coefficient of $(4 \pm 1) \times 10^{-14}\,cm^3\,molec^{-1}\,sec^{-1}$ for the quenching of the emission by OCS in both liquid media. It must reflect a combination of quenching both the free and bound $S(^1S)$. This is approximately an order of magnitude smaller than the $(4 \pm 2) \times 10^{-13}\,cm^3\,molec^{-1}\,sec^{-1}$ determined for the quenching of $S(^1S)$ by OCS at room temperature[7] after allowing for the effects of H_2S and CS_2 impurities. This reduced value may result from most of the $S(^1S)$ being bound up as $2\,^1\Sigma^+$ molecues, and these molecules being less effectively quenched by OCS (or impurities it contains). It may also be a temperature dependence of the rate coefficient for the $S(^1S)$ - OCS interaction as observed for $O(^1S)$ quenching by N_2O.[11]

Acknowledgements

REFERENCES

1. G. Black, R. L. Sharpless, T. G. Slanger, and D. C. Lorents, J. Chem. Phys. <u>62</u>, 4274 (1975).

2. G. Black, R. L. Sharpless, and T. G. Slanger, J. Chem. Phys. <u>63</u>, 4551 (1975).

3. G. Black, R. L. Sharpless, and T. G. Slanger, J. Chem. Phys. <u>69</u>, 794 (1978).

4. G. Black and R. L. Sharpless, J. Chem. Phys. <u>70</u>, 5571 (1979).

5. R. J. Donovan, Trans. Faraday Soc. <u>65</u>, 1419 (1969).

6. R. J. Donovan, L. J. Kirsch and D. Husain, Trans. Faraday Soc. <u>66</u>, 774 (1970).

7. O. J. Dunn, S. V. Filseth and R. A. Young, J. Chem. Phys. <u>59</u>, 2892 (1973).

8. J M. Brom, Jr., and E. J. Lepak, Chem. Phys. Lett. <u>41</u>, 185 (1976).

9. J. Fournier, C. Lalo, J. Deson and C. Vermeil, J. Chem. Phys. <u>66</u>, 2656 (1977).

10. J. A. Margevicius, M. V. McCusker, L. Abouaf, D. C. Lorents, and D. L. Huestis, "Optical Emissions from Doped Condensed Rare Gases Excited by Electrons," presented at the 30th Gaseous Electronics Conference, Palo Alto, California, 18-21 October 1977; "ArS, XeO, and ArO Emissions for Liquid Argon Hosts: Spectra and Kinetics,"

presented at the Tenth International Quantum Electronics Conference, Atlanta, Georgia, 29 May - 1 June, 1978.

11. G. Black and R. L. Sharpless, J. Chem. Phys. $\underline{71}$, (1979) [previous paper].

12. P. S. Julienne, M. Krauss and W. Stevens, Chem. Phys. Lett. $\underline{38}$, 374 (1976).

13. P. S. Julienne, J. Chem. Phys. $\underline{68}$, 32 (1978).

FIGURE CAPTIONS

Fig. 1   Emissions following the production of $S(^1S)$ from OCS photo-

dissociation in the wavelength region 140 - 161 nm, in both

liquid argon ($88^\circ K$) and liquid nitrogen ($77^\circ K$). OCS = 0.35 ppm.

Asterisks indicate scattered light from the H_2 photolysis

lamp.

Fig. 2   Decay of $S(^1S)$ in liquid N_2 ($77^\circ K$) containing [OCS] =

$0.27 \times 10^{16} \, cm^{-3}$. Three min. experiment at λ = 158 nm.

Fig. 3   Decay rate of $S(^1S)$ vs. [OCS] in liquid argon ($88^\circ K$) and

liquid N_2 ($77^\circ K$).
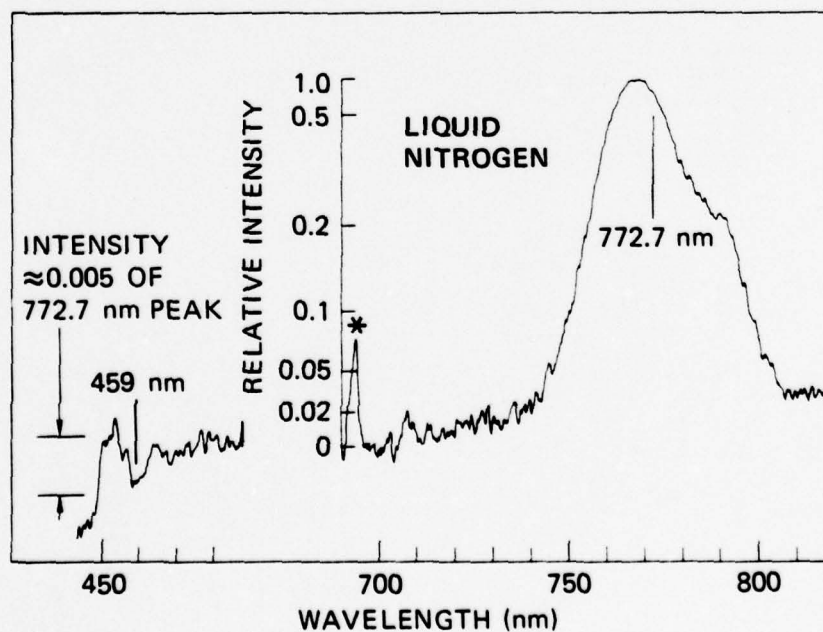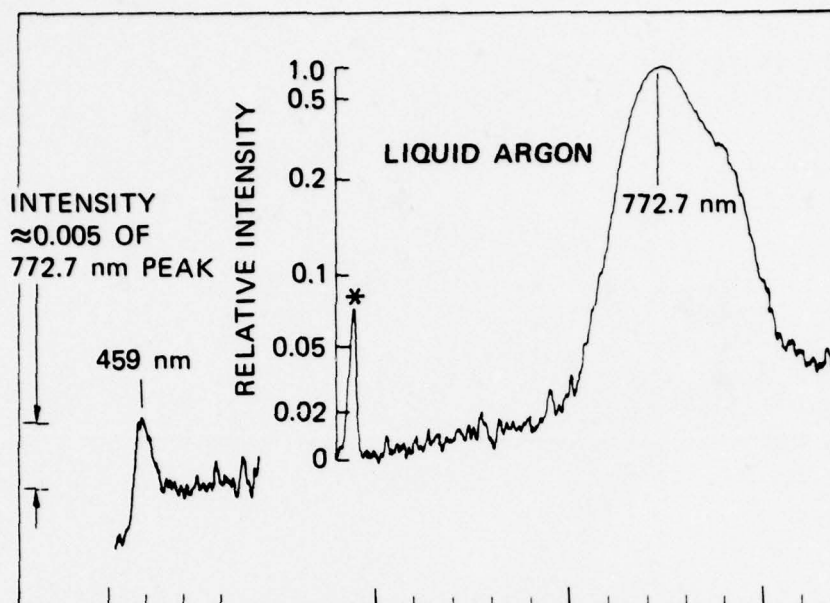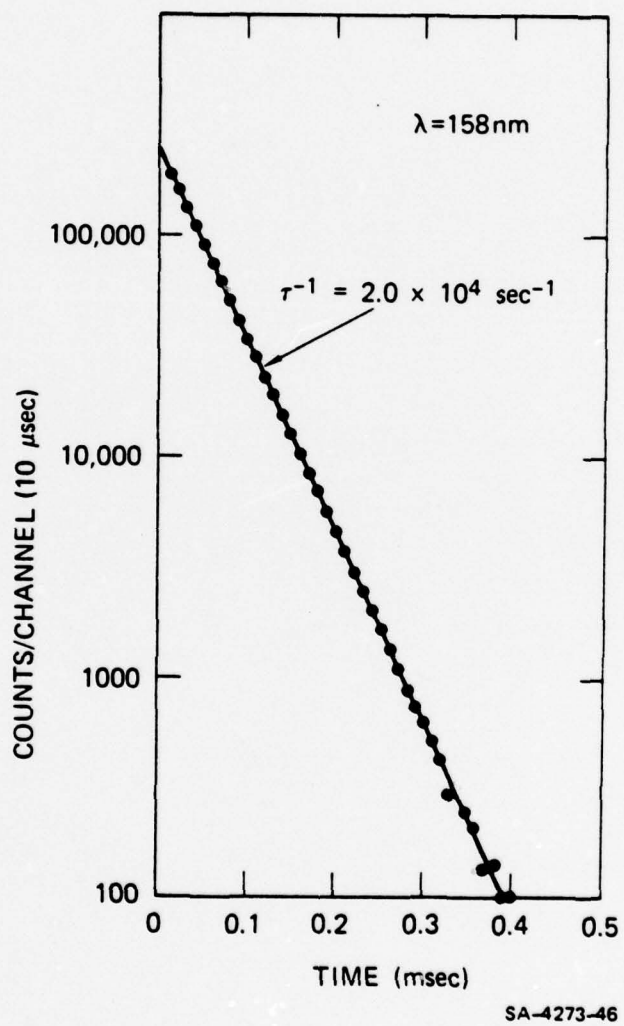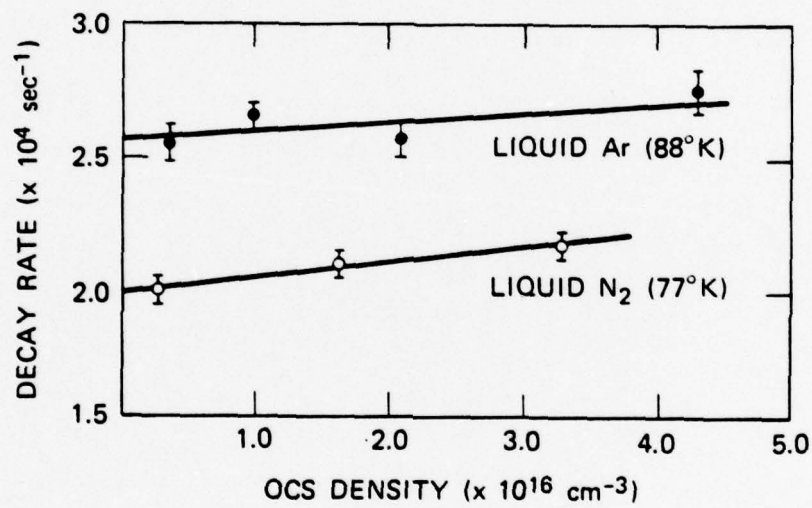
Figure 1

SA-4273-51

Figure 2

SA-4273-46

Figure 3

Appendix D

XeF$_2$ PHOTODISSOCIATION STUDIES.
I. QUANTUM YIELDS AND KINETICS OF XeF(B) AND XeF(C)

G. Black, R. L. Sharpless, D. C. Lorents, and D. L. Huestis
SRI International, Menlo Park, CA 94025

R. Gutcheck[*]
Stanford Synchrotron Radiation Laboratory
Menlo Park, CA 94025

T. Bonifield, D. Helms, and G. K. Walters
Rice University, Houston, TX 77001

ABSTRACT

Photodissociation of XeF$_2$ with synchrotron light pulses (0.3 nsec
duration) has been used as the source of XeF(B, C, and D) states. The
intensity-time profiles of the resulting fluorescence have been recorded
and analyzed. Most of the measurements were carried out in the strong
absorption band between 145 and 175 nm for which a peak absorption
coefficient of 1450 ± 150 cm^{-1}atm^{-1} (at 158 nm) was determined. By
comparison with O(^{1}S) signals from N$_2$O, quantum yields for B, C, and D
state production were determined. Radiative lifetimes of (13 ± 1) nsec
and (100 ± 10) nsec were found for the B and C states. Rate coefficients
for quenching both states by XeF$_2$ and for converting B to C are reported
for Ne, Ar, and N$_2$ as well as upper limits on quenching the C state by
these gases.

[*]Present address: SRI International, Menlo Park, CA 94025

INTRODUCTION

The XeF laser, operating on the B → X transitions at 351 and 353 nm and on the C → A transition at 483 nm,[1] provides the longest wavelengths of the uv rare gas halide lasers and has been the subject of considerable investigation. In electron-beam pumped $Ne/Xe/NF_3$ mixtures, substantial output energies have been obtained at reasonable efficiencies--the highest reported to date being 5.5%.[2] However, this efficiency is still well below the theoretical maximum of 13% based on the ratio of the 3.5 eV XeF photon to the 27 eV primary excitation energy in neon. To achieve the best possible laser performance, it is necessary to understand in detail the kinetics of the numerous processes occurring in the laser medium.

These processes have been much studied using both e-beam excitation[3-6] and photodissociation[7-11] of XeF_2 as sources of electronically excited XeF. In addition, a recent study[12] utilized direct optical pumping of ground state XeF molecules to XeF(B)[13] using a XeF laser pulse. Direct observation of the XeF(B → X) emission at ≈ 350 nm has been used to determine the radiative lifetime of XeF(B) and the collisional rate coefficients. The latter have also been deduced[9] from a Stern-Volmer analysis of the XeF(B → X) and XeF(C → A) emission intensities produced in the steady state photolysis of XeF_2. Although there is reasonable agreement on the radiative lifetime of XeF(B)--most values falling within the range (16.0 ± 2.0) nsec, considerable disagreement exists on the relative roles played by two-body and three-body removal of XeF(B).

The XeF(C) state, emitting a broad continuum between ~ 390 and 550 nm, is much less studied in large part because of complications arising from its collisional mixing with XeF(B) and because photodissociation of XeF_2 produces very little XeF(C)--at least for $\lambda > 145$ nm. A further difficulty may arise from the presence of B $\rightarrow$ A emission in the same spectral region. Very recently short-pulse electron impact dissociation of XeF_2 has been used to determine a radiative lifetime of (93 ± 5) nsec for XeF(C) in reasonable agreement with the measurement of 80 nsec by Center[14] and the theoretical value of 113 nsec by Dunning and Hay.[15] Most of the rate coefficient information on the XeF(C) state has been deduced[9] from emission intensity measurements in the steady-state photolysis of XeF_2. Measurements in such a system and in two separate experiments in this laboratory[16,17] have also established that there is ~ 600 cm^{-1} energy separation between the B and C states (based on 6.5 as the ratio of the radiative lifetimes of the C and B states).

The work to be described here utilizes photodissociation of XeF_2 with wavelength resolved synchrotron radiation to produce the B and C (and D) states. The very narrow pulse duration (0.3 nsec) provides an order of magnitude improvement in time resolution over previous measurements. This has allowed kinetic measurements to be carried out at much higher gas pressures. We also report the first quantum yield measurements on the B, C, and D states in the 145 to 175 nm absorption region.

As with most of the previous measurements, the results to be reported represent an average over a particular distribution of vibrational levels

in the excited state (involving a convolution of the excited state distribution produced and the filter transmission characteristics). It will be shown that vibrational relaxation from high levels of the XeF(B) state to the low vibrational levels observed in the present (and most previous) experiments can play an important role in determining XeF(B) state kinetics. It appears that this effect may be responsible for the quenching behavior observed in previous work and attributed to a combination of two- and three-body quenching. In the present work we find no evidence for three-body quenching of the XeF(B) state by Ne, Ar. or N_2.

EXPERIMENTAL

These measurements have been performed on the 8° Beamline at the Stanford Synchrotron Research Project using the synchrotron radiation from the SPEAR storage ring at the Stanford Linear Accelerator Center. This light source provides unique timing capabilities since the pulse duration is 0.3 nsec and repeats at 1.28 MHz. Photodissociation of XeF_2 at $\lambda < 200$ nm has been used as the source of electronically excited XeF (B, C, and D) states. Most of the work has been performed between 145 and 175 nm where XeF_2 exhibits a strong absorption band ($f \approx 0.4$--see later).

All the timing experiments were taken with the conventional Time-to-Amplitude Converter (TAC) system using the fluorescence photon as the start signal and the exciting light pulse as the stop signal. Details of the experimental cell, which incorporates three MgF_2 windows, have been

given elsewhere.[18] The fluorescence was measured with an EMI 9813QAM looking through a 350 nm interference filter (15 nm FWHM) for the XeF(B) emission and a Wratten 2E filter for the XeF(C) emission. A few measurements were also made on the XeF(D) state using a 254 nm filter with 13 nm FWHM to observe the D → X emission. The response time of the photomultiplier-TAC system was ~ 0.8 nsec.

In addition to serving as the start channel on the TAC system, the fluorescence signal was also measured with a ratemeter and displayed on one channel of a two-channel pen recorder. The intensity of the exciting synchrotron radiation was monitored by a sodium salicylate disc-photomultiplier combination whose output was measured on a Hewlett-Packard micro-microammeter and displayed on the second channel of the two-channel pen recorder. The pen recorder would then display an absorption-excitation spectrum when the monochromator was scanned. Furthermore the absolute synchrotron flux as a function of wavelength was determined with a calibrated vacuum uv photodiode. This enabled the response of the salicylate disc with wavelength to be determined[19] and its constancy checked several times during the experiment.

The XeF_2 was purchased from PCR Research Chemicals Inc. The Ne, Ar, and N_2 were all of ultra high purity grade. All pressures were measured on Baratron pressure transducers. The XeF_2 was pumped on prior to each use to remove the products of its slow decomposition (perhaps arising from wall reactions in its pyrex containing vessel). Gases were mixed

in a stainless steel vessel prior to introduction into the photolysis cell.

Quantum yields were measured by comparison to the $O(^1S)$ signal from N_2O photolysis for which the quantum yield is known.[19,20] The latter measurement utilized a N_2O/Xe mixture containing 1 torr N_2O and 1420 torr of Xe in which 25% of the $O(^1S)$ radiates.[19,21] It was made using the same photomultiplier and the Wratten 2E filter and simply recording the fluorescence signal (counts/sec) and the absorption of the N_2O/Xe sample as the monochromator was scanned. This trace was then compared to those obtained using only XeF_2 in the photolysis cell, at pressures in the range 0.3-3.5 torr, and the filters for the B, C, and D state emissions.

RESULTS

A. XeF$_2$ Absorption Cross Section

From the absorption spectra as a function of XeF_2 pressure we were able to determine a value of 1450 ± 150 cm^{-1}atmos^{-1} for the value of the XeF_2 absorption coefficient at the 158 nm peak. For the whole band an f-value of ≈ 0.4 was determined. The peak absorption cross section is slightly more than a factor of two smaller than the earlier reported value of Nielson and Schwarz.[22] The reason for this discrepancy is unknown but a similar situation has been found to exist at 172 nm in previous measurements in this laboratory[1] (although in this case a factor of four discrepancy was measured).

Quantum Yields

The intensity of the XeF(B) state fluorescence, at XeF_2 pressures of 3.5, 1.0, and 0.3 torr, is shown as a function of photolysis wavelength in Figure 1. The double humped curve (peaks at 147 and 170 nm) with XeF_2 = 3.5 torr reflects the effect of optical thickness--at this pressure, in the center of the absorption band, most of the absorption occurs close to the entrance window and the resulting fluorescence is not efficiently measured. The peaks appear when the optical density provides the maximum absorption (and hence fluorescence--assuming a constant quantum yield) in the region viewed by the EMI 9813QAM photomultiplier. The relative heights of the two peaks closely reflect the relative photolysis intensities at 147 and 170 nm indicating that, within 10%, the quantum yield of XeF(B) state production is the same at these two wavelengths. As the XeF_2 pressure is lowered the two peaks move together and finally, at XeF_2 = 0.3 torr, merge to a single peak which appears at the peak of the XeF_2 absorption (158 nm).

For the quantum yield determination the peak signal obtained with XeF_2 at 1.0 torr of $\sim$ 6700 sec^{-1} was compared with the peak signal of $\sim$ 12000 sec^{-1} obtained for $XeO(^1S)$ with the N_2O/Xe mix (this occurred at $\sim$ 132.5 nm when the N_2O absorption cross section is approximately the same as that of XeF_2 at 165 nm). The $XeO(^1S)$ trace showed only the single peak at this wavelength because of Xe absorption (as Xe_2) below 132 nm. At 1 torr XeF_2, 82% of the XeF(B) radiates (see later) compared

to 25% for the XeO(^{1}S). Furthermore the flux at 165 nm was 0.18 times

the flux at 132.5 nm (because of narrower slits at 165 nm). The filter

transmission for the XeF(B) state emission is estimated at 15% compared

to 90% for the XeO(^{1}S) emission. The quantum efficiency of the photo-

multiplier decreases from 27% at 350 nm (the XeF(B) emission) to 5.6% at

540 nm (although the XeO(^{1}S) emission extends[23] from > 560 to < 500 nm).

Using 0.96 as the O(^{1}S) yield from N_2O at 132.5 nm then gives 0.97 for

the XeF(B) yield. In view of the numerous sources of error and the

~ 0.08 yield of XeF(C) state (see below), the B state yield at 165 nm

is $0.9 {+0.1 \atop -0.2}$. Furthermore, correcting for the XeF_2 quenching in traces

like Figure 1(a) indicates that this holds over the 146 to 172 nm range.

In a similar measurement of the yield of XeF(C) state using the

Wratten 2E filter it was found that the light transmitted by this filter

corresponded to a quantum yield of 0.11. However in this region the B → A

emission contributes[15] approximately 0.03. Hence the XeF(C) state yield

is ~ 0.08 at 157.5 nm (with an estimated uncertainty of ± 0.02) and

decreases by ~ 40% between 146 and 172 nm. This is consistent with

previous work[9] using both Hg (184.9 nm) and CO (160-180 nm) lamps which

found that the C state yield was more than an order of magnitude less

than the B state yield.

We also find a XeF(D) state quantum yield of 0.028 ± 0.005 at 155 nm

which decreases by at least a factor of 2 in going to 165 nm.

KINETIC RESULTS

A. **XeF$_2$ Alone (No Buffer Gas)**

With no buffer gas, a plot of τ^{-1} of the XeF(B) state emission vs

XeF$_2$ gave an intercept of (13 ± 1.5) nsec for the radiative lifetime of

XeF(B) and a slope of $(5.5 \pm 1.0) \times 10^{-10}$ cm^3 molec^{-1} sec^{-1} for the

quenching of XeF(B) by XeF$_2$. Previous measurements of the radiative

lifetime range from (13.5 ± 1.0) nsec[24] to (19.4 ± 1.0) nsec[12]--the latter

being for the v'=0 level and hence the present value is in satisfactory

agreement, bearing in mind that different vibrational distributions may

be involved in each experiment. The quenching rate coefficient is

approximately a factor of two higher than the $(2.6 \pm 0.3) \times 10^{-10}$ cm^3 molec^{-1} sec^{-1}

reported by Eden and Waynant[10] and still substantially higher than the

3.5×10^{-10} cm^3 molec^{-1} sec^{-1} reported by Burnham and Harris.[7] The reason

for this disagreement is not known.

Similar measurements on the XeF(C) state in the absence of any

buffer gas were not attempted because of the two component decays

presumably coming from the presence of both B $\rightarrow$ A and C $\rightarrow$ A emissions.

Quenching measurements on the XeF(D) state will be reported later.

B. **XeF(B) State with Ne, Ar, and N$_2$ Buffer Gases**

In the presence of a buffer gas, the XeF(B) state emission has a

two-component decay due to mixing with the XeF(C) state. Typical

intensity-time plots of the XeF(B) and XeF(C) state emissions are shown

in Figure 2. It can also be seen that the rise time of the XeF(C) state

emission is much longer than that of the XeF(B) state emission (and, in

fact, has a rise time approximating the decay time of the XeF(B) emission)

as expected when the major source of the XeF(C) state involves collisional production from the XeF(B) state. The decay of the XeF(B) emission was fitted with two exponentials. The fast decay as a function of buffer gas pressure is shown for Ar, Ne, and N_2 in Figures 3, 4, and 5. A slight correction (in all cases < 20%) to the fastest decays shown was necessitated by the response time of the electronics ($\approx$ 0.8 nsec). The necessary deconvolution techniques to make this correction are presently being refined and will be applied to even faster decays in the near future. In all cases a line is shown connecting a value of $7.6 \times 10^7 \text{ sec}^{-1}$ on the intercept (the reciprocal of the radiative lifetime, $\tau_R(B)$, measured earlier) and the highest decay rates observed. This was done because, at low buffer gas additions, lifetimes longer than $\tau_R(B)$ were observed. This indicates that low buffer gas additions provide an additional source of the emissions being observed through the 350 nm filter on the same time scale as the measured decay. Since the filter transmits light mainly from low vibrational levels of the XeF(B) state it seems likely that this additional source involves vibrational relaxation from the high levels not seen to the low vibrational levels transmitted by the filter. Spectral evidence for the production of high vibrational levels has been reported previously.[8] We can rule out the XeF(D) state as the source of XeF(B) because of its small quantum yield. The observed behavior indicates that the efficiency of vibrational relaxation increases in the order Ne, Ar, and N_2 as would be expected. Previous studies in these systems (but limited

to slower decay rates and hence smaller buffer gas additions) have explained similar behavior by the occurrence of both two- and three-body quenching. We do not find any evidence for three-body quenching, and feel that vibrational relaxation is probably also involved in the previous studies. The slopes of the line in Figures 3, 4, and 5 correspond to rate coefficients of $(1.0 \pm 0.1) \times 10^{-11}$, $(1.8 \pm 0.3) \times 10^{-12}$, and $(5.7 \pm 0.6) \times 10^{-11}$ $cm^3 molec^{-1} sec^{-1}$ for Ar, Ne, and N_2, respectively (after correcting for the small XeF_2 contribution).

Because of the collisional mixing of the B and C states, the significance of these rate coefficients requires further consideration. If we represent the mixing process by

$$XeF(B) + Rg \underset{k_{CB}}{\overset{k_{BC}}{\rightleftharpoons}} XeF(C) + Rg$$
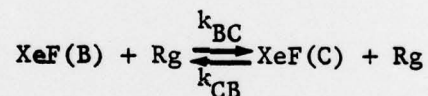
then the B state can be represented as the sum of two exponentials

$$B = b_1 e^{-\lambda_1 t} + b_2 e^{-\lambda_2 t}$$

where
$$\lambda_{1,2} = \frac{\beta+\gamma}{2} \mp \frac{1}{2} \left[(\beta-\gamma)^2 + 4 k_{CB} k_{BC} Rg^2 \right]^{\frac{1}{2}}$$

where β and γ represent the total rate of B and C state removal, respectively

$$\beta = \tau_R^{-1}(B) + k_{XeF_2}(B)[XeF_2] + k_{BC}[Rg]$$

and
$$\gamma = \tau_R^{-1}(C) + k_{XeF_2}(C)[XeF_2] + k_{CB}[Rg] \quad .$$

From the earlier results we know $\tau_R(B)^{-1} = (7.6 \pm 0.7) \times 10^7$ sec^{-1} and $k_{XeF_2}(B) = (5.5 \pm 1.0) \times 10^{-10}$ cm^{3}molec^{-1}sec^{-1}. Also it will be shown below that $\tau_R^{-1}(C) = (1.0 \pm 0.1) \times 10^7$ sec^{-1} and $k_{XeF_2}(C) = (5.3 \pm 0.5) \times 10^{-10}$ cm^{3}molec^{-1}sec^{-1}. Since the energy separation of the B and C states[4] is (610 ± 60) cm^{-1} we also know that $k_{CB} = (0.056 \pm 0.016)$ k_{BC}. k_{BC} was therefore used as the adjustable parameter to calculate values of λ_1 and λ_2 to compare with the experimental results. In all cases it was found that, within the experimental error at high buffer gas pressures (where vibrational relaxation does not appear to effect the fast decay), λ_2 could be equated with β and hence the rate coefficients quoted for Ar, Ne, and N$_2$ refer to k_{BC}. These rate coefficients could also include contributions from direct quenching of XeF(B) [to give products other than XeF(C)], but based on the previous work[9] this contribution is expected to be negligible. These values are approximately a factor of two larger than those reported in two previous studies.[9,10] In the case of the steady-state measurements[9] this difference arises, at least in part, from ignoring the rapid quenching of XeF(C) by the XeF$_2$ present in those experiments. In the previous time-resolved fluorescence studies,[10] the inclusion of three-body quenching causes underestimation of the two-body rate coefficient.

C. <u>XeF(C) Quenching</u>

Figure 6 shows the values of the decay rates of the XeF(C) state (and the slow component of the XeF(B) state) vs XeF$_2$ in argon buffer.

The argon pressure change of almost a factor of ten produces no significant change in the decay rate. This indicates that there is no quenching (rate coefficient $\leq 5 \times 10^{-14}$ $cm^3 molec^{-1} sec^{-1}$) of the XeF(C) state (as distinct from mixing with the XeF(B) state). It should be remembered that rate coefficients deduced from the value of λ_1 (the slow component of the B state decay), when a high buffer gas pressure provides rapid mixing of the B and C states, really relate to mixtures of $\approx 95\%$ C state and $\approx 5\%$ B state. It was found that the data shown in Figure 6 required a radiative lifetime of $(1.0 \pm 0.1) \times 10^7$ sec^{-1} for the XeF(C) state and $(5.3 \pm 0.5) \times 10^{-11}$ $cm^3 molec^{-1} sec^{-1}$ for its quenching by XeF_2. These values were also consistent with the more limited data taken in Ne and N_2 (although the upper limit for quenching the C state by N_2 has to be raised to 10^{-13} $cm^3 molec^{-1} sec^{-1}$). These upper limits on quenching by Ar, Ne, and N_2 are substantially lower than previous estimates.[9] The radiative lifetime for the C state is in good agreement with recent work.[4,14,15] The only discrepancy with previous work, as with B state quenching, concerns the quenching by XeF_2 which is a factor of three higher than the recent measurement of Waynant and Eden.[4] This may indicate that, although buffer gas was avoided in these latter experiments to minimize collisional coupling between the B and C states, some mixing is still occurring (perhaps via electron collisions).

A more extensive analysis of the present data is in progress. Of particular interest are the ratio of the slow and fast components in the

B state and C state fluorescence yields. From these it is possible to refine the determination of the energy separation of the B and C states and to assess the contribution of direct quenching of these states by rare gases and N_2.

ACKNOWLEDGMENTS

REFERENCES

1. W. K. Bischel, H. H. Nakano, D. J. Eckstrom, R. M. Hill, D. L. Huestis, and D. C. Lorents, Appl. Phys. Lett. $\underline{34}$, 565 (1979).

2. J. C. Hsia, J. A. Mangano, J. H. Jacob, and M. Rokni, Appl. Phys. Lett. $\underline{34}$, 208 (1979).

3. J. G. Eden and S. K. Searles, Appl. Phys. Lett. $\underline{30}$, 287 (1977).

4. R. W. Waynant and J. G. Eden, IEEE J. Quantum Electron. $\underline{QE-15}$, 61 (1979).

5. M. Rokni, J. H. Jacob, J. A. Mangano, and R. Brochu, Appl. Phys. Lett. $\underline{30}$, 458 (1977).

6. M. Rokni, J. H. Jacob, J. A. Mangano, and R. Brochu, Appl. Phys. Lett. $\underline{32}$, 223 (1978).

7. R. Burnham and N. W. Harris, J. Chem. Phys. $\underline{66}$, 2742 (1977).

8. H. C. Brashears, Jr., D. W. Setser, and D. Desmarteau, Chem. Phys. Lett. $\underline{48}$, 84 (1977).

9. H. C. Brashears, Jr., and D. W. Setser, Appl. Phys. Lett. $\underline{33}$, 821 (1978).

10. J. G. Eden and R. W. Waynant, Optics Lett. $\underline{2}$, 13 (1978).

11. J. G. Eden and R. W. Waynant, J. Chem. Phys. $\underline{68}$, 2850 (1978).

12. C. H. Fisher and R. E. Center, J. Chem. Phys. $\underline{69}$, 2011 (1978).

13. The notation used in this paper to label the XeF electronic states is the same as that of J. Tellinghuisen, A. K. Hays, J. M. Hoffman, and G. C. Tisone, J. Chem. Phys. $\underline{65}$, 326 (1976).

14. R. E. Center, private communication.

15. T. H. Dunning, Jr., and P. J. Hay, J. Chem. Phys. $\underline{69}$, 134 (1978).

16. D. L. Huestis et al., SRI International Report No. MP 78-07, 1978 (unpublished).

17. D. Kligler, H. H. Nakano, D. L. Huestis, W. K. Bischel, R. M. Hill, and C. K. Rhodes, Appl. Phys. Lett. $\underline{33}$, 39 (1978).

18. T. Bonifield, D. Helms, G. K. Walters, D. C. Lorents, G. Black, R. L. Sharpless, and R. Gutcheck, "Radiative and Collisional Properties of the 1_u and 0_u^+ States of Xe_2," submitted to J. Chem. Phys.

19. G. Black, R. L. Sharpless, T. G. Slanger, and D. C. Lorents, J. Chem. Phys. $\underline{62}$, 4266 (1975).

20. M. J. McEwan, G. M. Lawrence, and H. M. Poland, J. Chem. Phys. $\underline{61}$, 2857 (1974).

21. G. Black, R. L. Sharpless, and T. G. Slanger, J. Chem. Phys. $\underline{63}$, 4546 (1975).

22. U. Nielsen and W.H.E. Schwarz, Chem. Phys. $\underline{13}$, 195 (1976).

23. G. Black, R. L. Sharpless, and T. G. Slanger, J. Chem. Phys. $\underline{69}$, 794 (1978).

24. J. J. Ewing, 7th Winter Colloquium on Quantum Electronics (Park City, Utah, 1977).

FIGURE CAPTIONS

Figure 1   XeF(B) fluorescence intensity at 350 nm vs photolysis wavelength at three XeF_2 pressures. During this set of measurements the photolysis beam intensity decreased by $\approx$ 10%.

Figure 2   Intensity-time plots of the XeF(B) and XeF(C) state emissions produced by XeF_2 photodissociation at 172 nm. Ar = 500 torr and XeF_2 = 0.36 torr. Only $\approx$ 10% of the data points are shown plotted.

Figure 3   The fast decay rate of the XeF(B) state emission at 350 nm vs pressure for an Ar + 710 ppm XeF_2 mixture.

Figure 4   The fast decay rate of the XeF(B) state emission at 350 nm vs pressure for a Ne + 770 ppm XeF_2 mixture.

Figure 5   The fast decay rate of the XeF(B) state emission at 350 nm vs pressure for N_2 + 2740 ppm XeF_2 mixture.

Figure 6   Decay rate of the XeF(C) state emission vs XeF_2 pressure in three different Ar/XeF_2 mixtures.
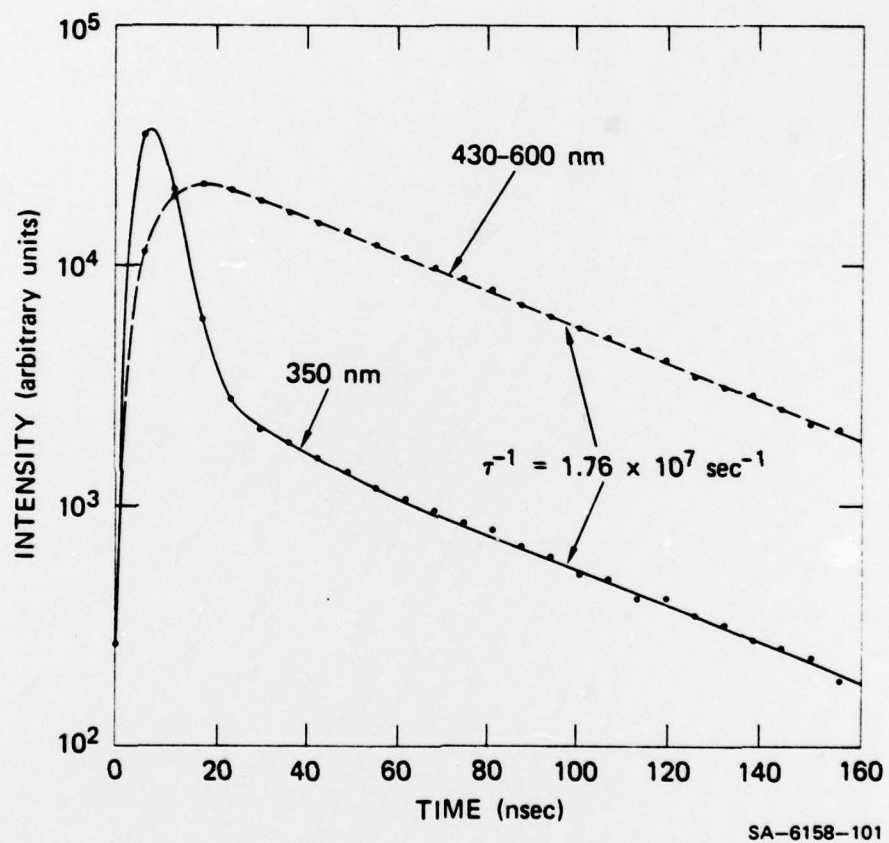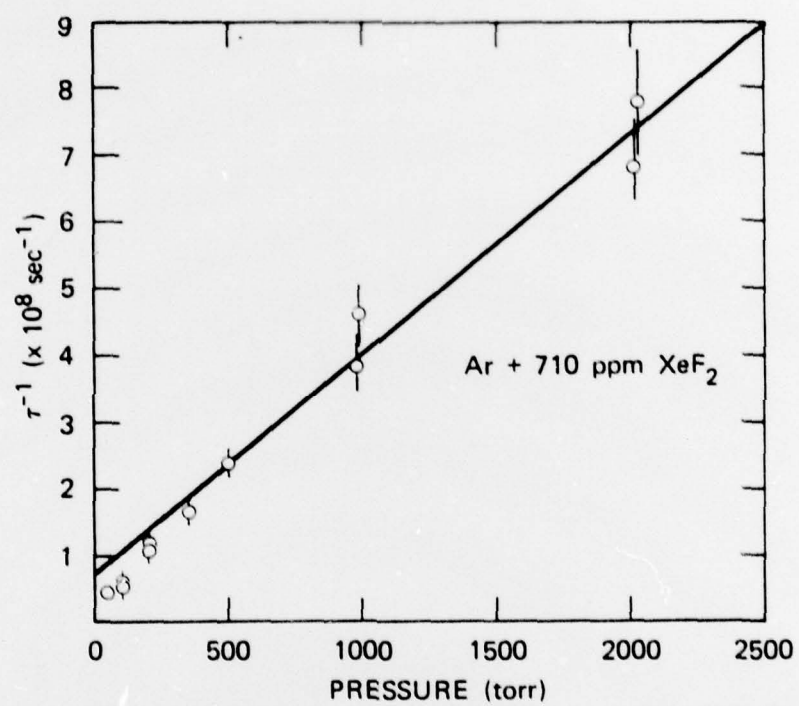
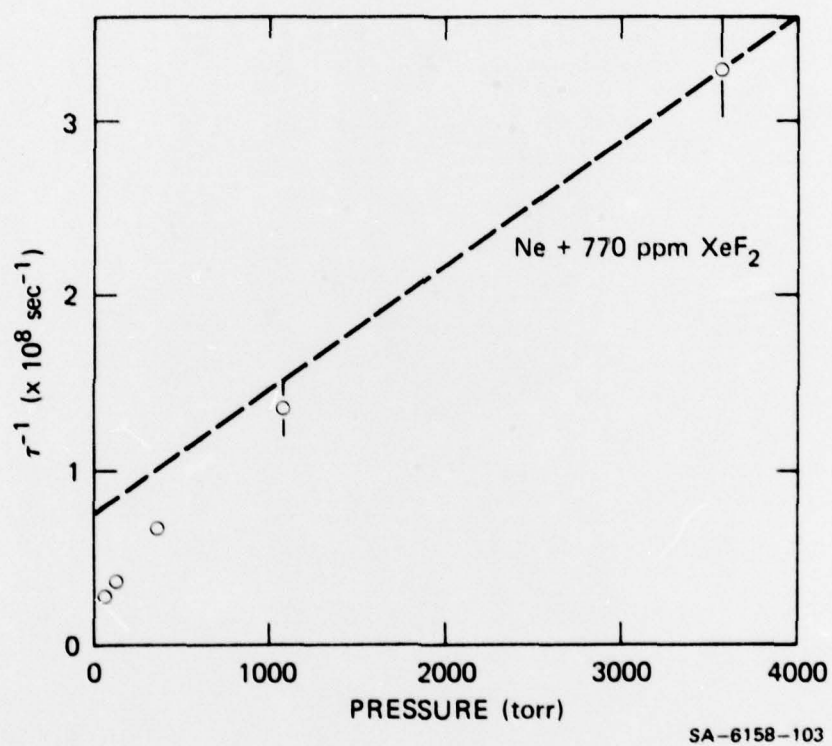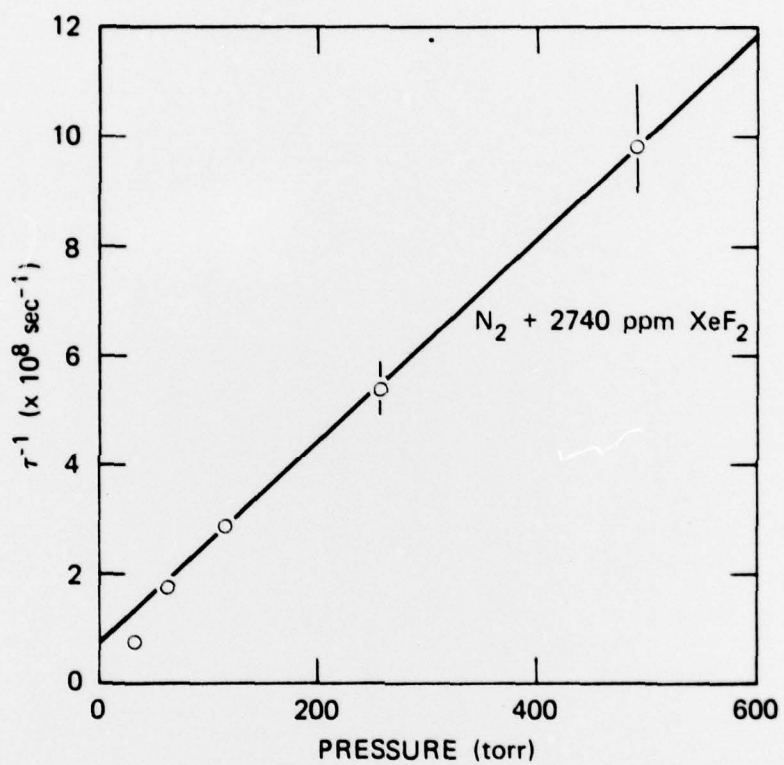Figure 1

D-18

Figure 2

SA-6158-101

D-19
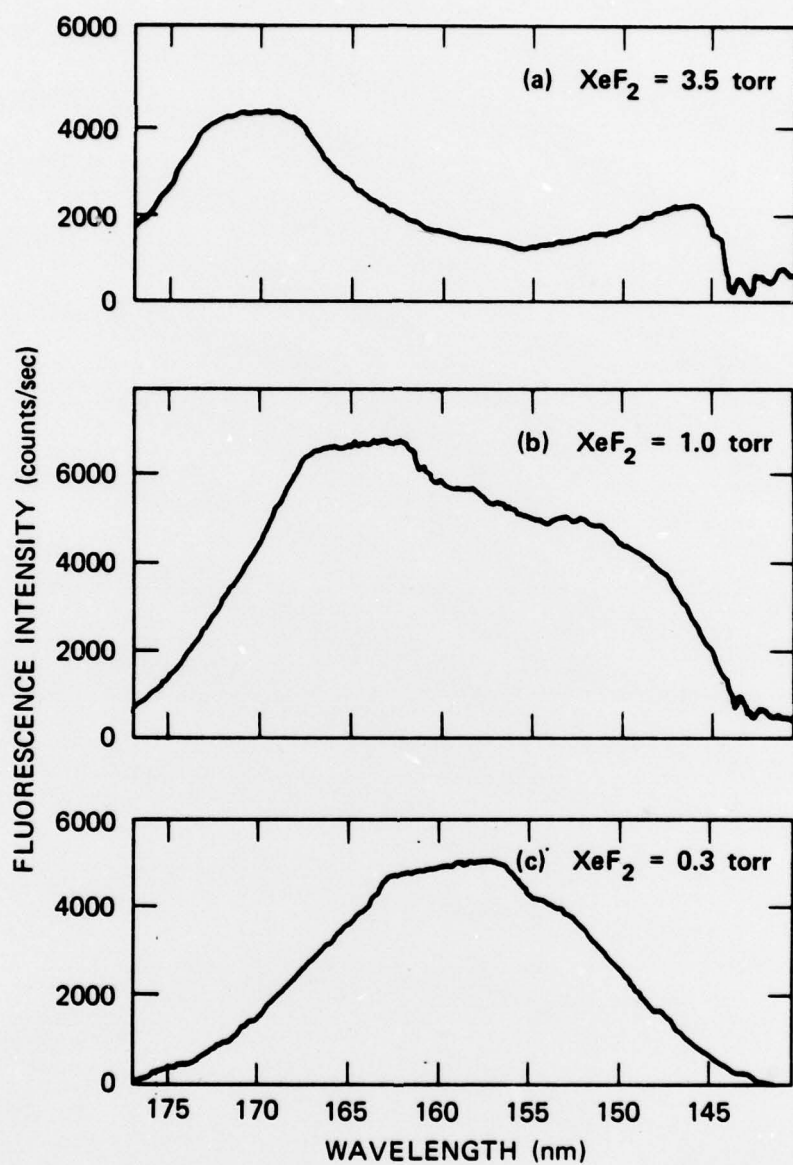
Figure 3

SA-6158-104

Figure 4

SA-6158-106

Figure 5

SA—6158—105

Figure 6